

2012

Melt Modulation Technology Enhancement For Molding Packing Stage Control Application

Punlop Teeraparpwong
Lehigh University

Follow this and additional works at: <http://preserve.lehigh.edu/etd>

Recommended Citation

Teeraparpwong, Punlop, "Melt Modulation Technology Enhancement For Molding Packing Stage Control Application" (2012). *Theses and Dissertations*. Paper 1244.

This Thesis is brought to you for free and open access by Lehigh Preserve. It has been accepted for inclusion in Theses and Dissertations by an authorized administrator of Lehigh Preserve. For more information, please contact preserve@lehigh.edu.

Melt Modulation Technology Enhancement
For Molding Packing Stage Control Applications

Punlop Teeraparpwong

A Thesis

Presented to the Graduate and Research Committee

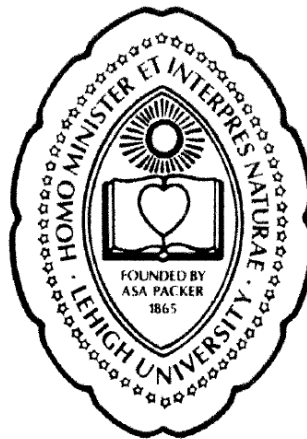
of Lehigh University

in Candidacy for the Degree of

Master of Science

in

Mechanical Engineering and Mechanics



Lehigh University

January 2012

CERTIFICATE OF APPROVAL

This Thesis is accepted and approved in partial fulfillment of the requirement for the
Master of Science in Mechanical Engineering and Mechanics.

Date

Dr. John P. Coulter, Thesis Advisor
Associate Dean of P.C. Rossin College of Engineering
Department of Mechanical Engineering and Mechanics

Dr. Gary Harlow
Department Chair
Department of Mechanical Engineering and Mechanics

TABLE OF CONTENTS

LIST OF TABLES.....	v
LIST OF FIGURE.....	vi
ABSTRACT	1
CHAPTER 1 – INTRODUCTION.....	3
1.1 Introduction to Melt Modulation System for Injection Molding Process.....	3
1.2 Motivation & Research Objectives.....	6
1.3 Thesis Outline.....	11
CHAPTER 2 – RELATED BACKGROUND.....	13
2.1 The Concept of Original Melt Modulation Technique	13
2.2 Control Valve Fundamental.....	15
2.3 Pressure Drop in a Cold Runner System	18
2.4 Compact Melt Modulation System.....	20
2.4.1 Control Valve	20
2.4.2 Driving Mechanism	23
2.4.3 Controller.....	25
2.4.4 Control Technique	27
2.4.5 Flow Characteristic Results and Discussion.....	30
2.5 Polymer Birefringence.....	35
2.6 Plastic Optics Quality	37
2.7 Limitation and Challenges.....	40
CHAPTER 3 – The Effect of Processing Parameters on the Properties of Injection- Molded Product	42
3.1 Introduction	42
3.2 Numerical Simulation.....	44
3.2.1 Average Volumetric Shrinkage	47
3.2.2 Deflection	49
3.2.3 Part Mass	51

3.3 Experimental Investigation.....	53
3.3.1 Birefringence	55
3.3.2 Tensile Testing	58
3.4 Discussion & Conclusion	60
CHAPTER 4 – Design of a Compact Melt Modulation System for Packing Stage	
Control Applications	62
4.1 Introduction	62
4.2 New Melt Modulation System Details	64
4.2.1 Mold insert.....	64
4.2.2 Actuator System	68
4.2.3 Valve Port.....	71
4.3 Conclusion.....	74
CHAPTER 5 – Design of Experiment and Numerical Simulation of Valve-runner	
System with Lens-shaped cavity.....	75
5.1 Introduction	75
5.2 Design of Experiment.....	76
5.3 Numerical Simulation Setup.....	80
5.4 Numerical Simulation Result.....	83
5.4.1 Different valve angle	83
5.4.2 Different packing pressure.....	85
5.4.3 Pressure at the cavity entrance.....	87
5.4.4 Average volumetric shrinkage.....	89
5.5 Discussion & Conclusion	90
CHAPTER 6 – SUMMARY AND CONCLUSION.....	91
6.1 Research Summary	91
6.2 Proposed Future Work.....	94
6.3 Conclusion Remarks.....	96
REFERENCES	98
VITA	101

LIST OF TABLES

Table 2-1 Design parameters for valve selection	21
Table 2-2 Original valve stem information	22
Table 2-3 Technical data of compact melt modulation system actuator	24
Table 2-4 Specification of gear mechanism for compact melt modulation design.....	25
Table 2-5 Photoelastic coefficient of polymer	37
Table 3-1 Injection unit specifications of Nissei machine.....	44
Table 3-2 Parameters used for numerical simulation	45
Table 3-3 L9 (3 ⁴) Orthogonal array	46
Table 3-4 Recommended processing conditions for polystyrene	54
Table 3-5 Parameters used for the experiment	54
Table 3-6 Modified L9 (3 ⁴) Orthogonal array	54
Table 4-1 Technical data of pressure transducer model 6159A	65
Table 4-2 Parameters of eccentric valve port	74
Table 5-1 Recommended processing parameters of PMMA, PC, and PS.....	76

LIST OF FIGURES

Figure 1-1 A failure during a filling process for family molding	4
Figure 1-2 Basic diagram of melt modulation technique	5
Figure 1-3 The completely filled parts produced with melt modulation technique	5
Figure 1-4 Actual melt modulation prototype	6
Figure 1-5 Conceptual CAD model of first melt modulation system	7
Figure 1-6 Pressure diagram of injection molding cycle	8
Figure 2-1 Rotary plug valve used with the runner	14
Figure 2-2 A traditional operation sequence of melt modulation system	14
Figure 2-3 Range of inherent flow characteristics for different control valves	16
Figure 2-4 Shifting of flow behavior due to reduced pressure ratio	17
Figure 2-5 Traditional control method for two valves system	18
Figure 2-6 Flow behavior of original melt modulation system	18
Figure 2-7 Shape factor	19
Figure 2-8 Full-round, parabolic, trapezoidal runner	19
Figure 2-9 Original valve stem design	21
Figure 2-10 Actual valve stem with ejector pin	22
Figure 2-11 Actuator used in compact melt modulation system	23
Figure 2-12 A prototype of compact melt modulation valve driving unit	25
Figure 2-13 PD control diagram for the actuator	26
Figure 2-14 USB controller for the compact melt modulation system	26
Figure 2-15 A control diagram with LVDT	27
Figure 2-16 Valve return cycle for fixed-angle control method	28

Figure 2-17 A timing diagram of Bang-Bang control method	29
Figure 2-18 A timing diagram of Hybrid control method	30
Figure 2-19 Spiral cavity drawing for the compact melt modulation evaluation	31
Figure 2-20 Spiral cavities layout	32
Figure 2-21 Valve characteristics using full port and 65% reduced port	33
Figure 2-22 Flow characteristic of Bang-Bang and Hybrid method from different valve port	34
Figure 2-23 A comparison between three control methods	34
Figure 2-24 Schematic of plane polarize scope activity	36
Figure 3-1 ASTM - D638 Type I dimension in millimeter	42
Figure 3-2 ASTM mold cavities	43
Figure 3-3 Nissei machine model PS40E5ASE	43
Figure 3-4 3D meshed model in MOLDFLOW	45
Figure 3-5 Gate and nodes position	46
Figure 3-6 Average volumetric shrinkage result for PMMA dog bone (Numerical)	47
Figure 3-7 Average volumetric shrinkage result for PC dog bone (Numerical)	48
Figure 3-8 Average volumetric shrinkage result for PS dog bone (Numerical)	48
Figure 3-9 Total deflection result of PMMA dog bone (Numerical)	50
Figure 3-10 Total deflection result of PC dog bone (Numerical)	50
Figure 3-11 Total deflection result of PS dog bone (Numerical)	51
Figure 3-12 Weight result of PMMA dog bone (Numerical)	52
Figure 3-13 Weight result of PC dog bone (Numerical)	52
Figure 3-14 Weight result of PS dog bone (Numerical)	53
Figure 3-15 Polarizer used in the experiment	55

Figure 3-16 Birefringence result from Taguchi L9 method	56
Figure 3-17 Retardation plot from the experiments.....	57
Figure 3-18 Maximum retardation result of PS dog bone (Experimental)	58
Figure 3-19 Tensile test equipment	59
Figure 3-20 Average maximum tensile load result of PS dog bone (Experimental)	59
Figure 3-21 Average maximum tensile stress result of PS dog bone (Experimental)	60
Figure 4-1 A-series mold base from DME Company	62
Figure 4-2 A-series mold base connected with a compact melt modulation system.....	63
Figure 4-3 Drawing of lens-shaped part	64
Figure 4-4 Kistler pressure transducer model 6159A	65
Figure 4-5 Pressure transducer position with the trapezoidal runner	66
Figure 4-6 Mold insert layout.....	67
Figure 4-7 Original compact system and the direct coupling valve design	68
Figure 4-8 Drawing of a valve coupler	69
Figure 4-9 Direct coupling valve design	69
Figure 4-10 New configuration of the compact system.....	70
Figure 4-11 Ideal performance and effective range of original valve ports	71
Figure 4-12 Eccentric valve port configuration.....	72
Figure 5-1 Cold runner system for packing stage control application.....	75
Figure 5-2 Packing profile of Nissei machine	77
Figure 5-3 Testing approach for packing pressure control.....	79
Figure 5-4 Testing approach for packing time control	79
Figure 5-5 The runner at control valve position of each model.....	81
Figure 5-6 25% model with 3D meshing.....	82

Figure 5-7 Pressure transducer positions	82
Figure 5-8 Pressure difference result of PMMA with four valve angles	83
Figure 5-9 Pressure difference result of PC with four valve angles	84
Figure 5-10 Pressure difference result of PS with four valve angles	84
Figure 5-11 Pressure difference result of PMMA with three levels of packing pressure	85
Figure 5-12 Pressure difference result of PC with three levels of packing pressure	86
Figure 5-13 Pressure difference result of PS with three levels of packing pressure	86
Figure 5-14 Pressure at the cavity entrance (PMMA)	87
Figure 5-15 Pressure at the cavity entrance (PC)	88
Figure 5-16 Pressure at the cavity entrance (PS)	88
Figure 5-17 Average volumetric shrinkage result at the center of the molded lens	89
Figure 6-1 The first compact system and the developed prototype	92
Figure 6-2 Developed configuration of the compact system	93
Figure 6-3 Valve position guideline for a new simulation	95

“You can’t connect the dots looking forward; you can only connect them looking backwards. So you have to trust that the dots will somehow connect in your future. You have to trust in something – your gut, destiny, life, karma, whatever. Because believing that the dots will connect down the road will give you the confidence to follow your heart even when it leads you off the well-worn path; and that will make all the difference.”

Steve Jobs

ABSTRACT

The melt modulation technique has been continuously improved in many aspects for a decade since its initial invention. The previous work has proved that the technology practically improved an injection molding process to the next level, including filling stage control of specific cavity and family molding. The primary goal of the research is to investigate and expand current Melt modulation capabilities to control the packing stage of cold runner based injection molding processes. Since packing parameters, including packing pressure and packing time, significantly contribute to the optical quality of injection molded polymeric products in terms of final geometry and optical isotropy, the investigation therefore focuses on controlling the packing stage in order to produce molded parts which have different optical properties. The polymers used throughout the research are common thermoplastic optical polymers, such as PMMA, PC, and PS. Together, the new Melt modulation configuration and mold equipment had been developed to work with this application.

The first phase of the research consisted of a set of numerical simulations and experiments with the purpose being to investigate the effect of various processing parameters on optical quality of standard dog-bone specimens. The results demonstrated that changing processing parameters, especially packing parameters significantly affects optical quality. The Melt modulation compact design was re-configured to be smaller, simpler for assembly, and to have more functionality. A cold runner mold which has two lens-shaped cavities was machined for a capability testing. A Pressure transducer was connected to the runner to monitor pressure affected by the control valve. The last phase was the design of an experiment for capability testing and numerical simulations. 3D models with four valve

angles were created according to the actual testing system previously fabricated. The simulation shows that pressure drops at the area after the control valve. However, valve angle is not an effective parameter to control pressure because it seems to have quick opening characteristic.

More investigation needs to be done in order to understand the capability of the control valve better while operating during the packing stage. The future works have been proposed before the research is summarized. The improvement of Melt modulation technique from this research and in the future will expand its benefit to the plastic industry.

CHAPTER 1 – INTRODUCTION

1.1 Introduction to Melt Modulation System for Injection Molding Process

At present, injection molding process is a major part of the plastics industry because of its ability to cope with complex parts, mass production, and excellent repeatability of molded products. The process has been developed since its invention until nowadays to correspond to a wide range of applications. Major types of injection molding systems classified by runner arrangement are hot runner and cold runner systems.

In the thermoplastic molding industry, cold runner systems dominate because of their many advantages over hot runner systems. Approximately 70% of molds used for molding thermoplastic materials are of the cold runner type [1]. The process used with cold runner system is by far the simplest as well; an injected material is filled in a runner profile, cooled, solidified and then ejected cavities every molding cycle. The major advantages of a cold runner system over a hot runner system are its simplicity to manage, operate, and maintain, and lower cost of mold construction. However, crucial design criteria with cold runner systems include gate positions and runner layout since a bad design can lead to poor product quality, such as deflection, undesirable weld lines, etc.

The injection molding process is commonly used for mass production due to its high speed of molding and good repeatability. To increase productivity, several improved designs can be applied to a mold. Family molding is one method used to mold parts with different sizes and shapes in the same mold and cycle. For some applications, this can help significantly reduce cost and production time. Family molding, however, is not widely used in industry due to difficulties in control of the process parameters for each part, such as

proper filling and packing. A case study is shown in Figure 1-1. Two types of electrical connectors were conventionally molded in the same shot of a cold runner system. Two small cavities on the left are completely filled while the larger cavities result in a “short shot” situation. The short shot occurs because the larger cavity requires more molten polymer than the smaller one. On the other hand, if one used more polymer to fill the larger cavities completely, it would exceed the capacity of the smaller, and will cause the smaller parts to “flash” or be “over-packed” during packing stage. By using melt modulation technology, patented by Lehigh University, the filling issue in family molding can be solved, i.e. all cavities are filled properly.

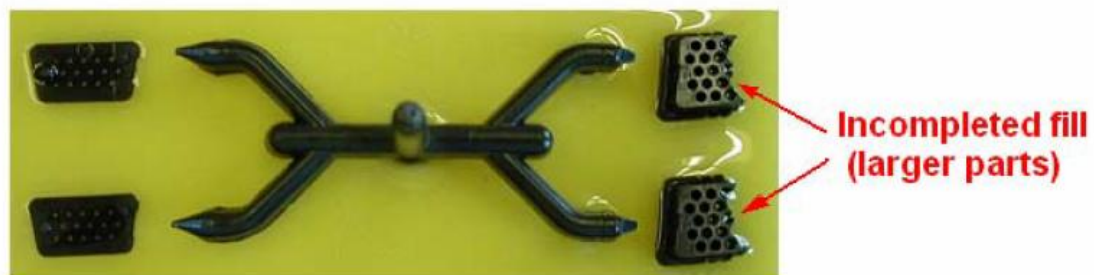


Figure 1-1 A failure during a filling process for family molding [2]

The concept of melt modulation is fairly simple. In order to control melt flow in a mold and fill the larger and smaller cavities properly in one cycle, a mechanical control valve is locally employed in the runner. The control valve rotates and adjusts a cross sectional area of a cold runner so that it can control the amount of polymer flowing to a certain mold region. The diagram describing a concept of the technique is shown in Figure 1-2. With such control valves implemented the problem in Figure 1-1 can be solved as presented in Figure 1-3

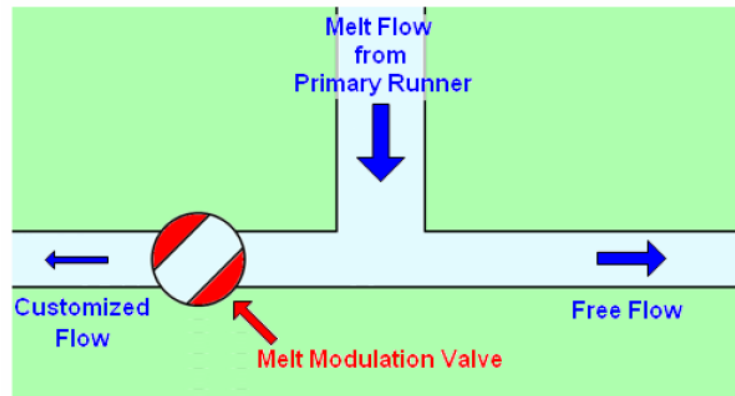


Figure 1-2 Basic diagram of melt modulation technique [2]



Figure 1-3 The completely filled parts produced with melt modulation technique [2]

First developed in 90's, the melt modulation technique has been continuously developed in order to make it more practical and efficient for cold runner system [2, 3]. Even though several applications have been dramatically improved with the control valves, potential of the melt modulation technique could still be expanded further. To improve its current ability, the melt modulation technique is investigated in the aspect of design and application in order to utilize it more widely.

1.2 Motivation & Research Objectives

Although the melt modulation system has proven its contribution to cold runner based injection molding, it is still not widely used because of its first impractical design in 90's as shown in Figures 1-4, and 1-5. The original model was designed in order to investigate the effect of a mechanical control valve on melt flow control, but efficiency, cost and practicality were not of primary concern. In addition, this model was restricted to only two control valves (due to limited space), and to a simple control technique, where one valve is left fully open and the other set at specific angle before injection. This made the original model too bulky, difficult to install, and too expensive for many machines in mass production. For these reasons, most manufacturers still use traditional solutions like retooling the mold, such as changing gate size and position, or changing runner layout.

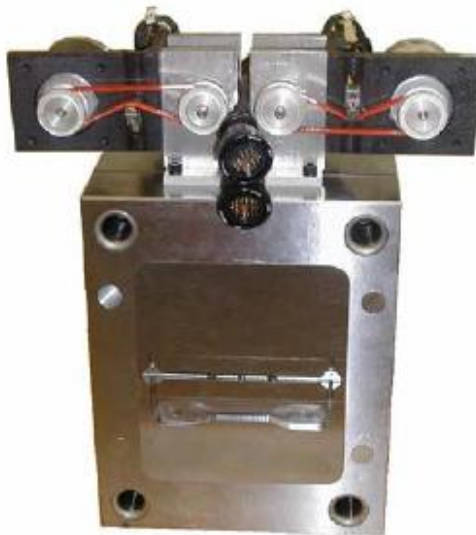


Figure 1-4 Actual melt modulation prototype [2]

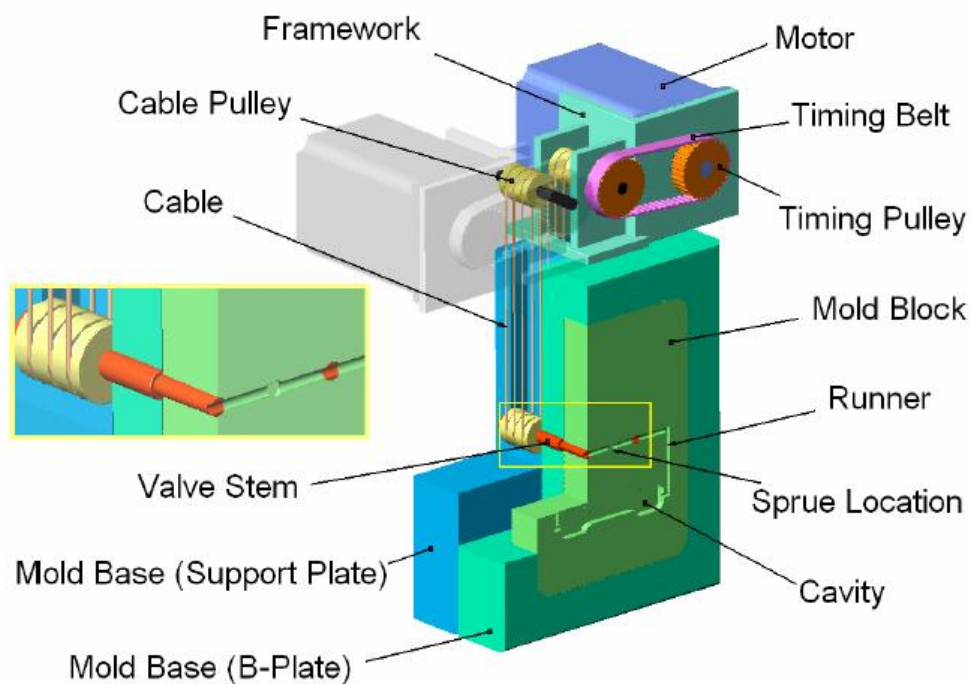


Figure 1-5 Conceptual CAD model of first melt modulation system [2]

Akapot Tantrapiwat, a former Lehigh Ph.D. student, studied the melt modulation technique for his dissertation titled “**Melt modulation systems for enhanced polymer processing**” [2] during 2005-2009. He totally re-designed the overall melt modulation system so that it yielded better performance, lower cost, and more practical application. More details of this related work will be presented in Chapter 2.

The pressure diagram of an injection molding cycle is shown in Figure 1-6. Both two previous melt modulation systems were focused on development and control of the filling stage (section I) of injection molding cycle for family molding, i.e. to balance the melt flow of different sizes and shapes cavities. The latest melt modulation system was found to produce excellent results for that purpose [2]. Now, the challenge is to expand the

application by utilizing mechanical control valves in the packing stage too (section II), in other words, trying to control packing pressure for each cavity by rotating a control valve.

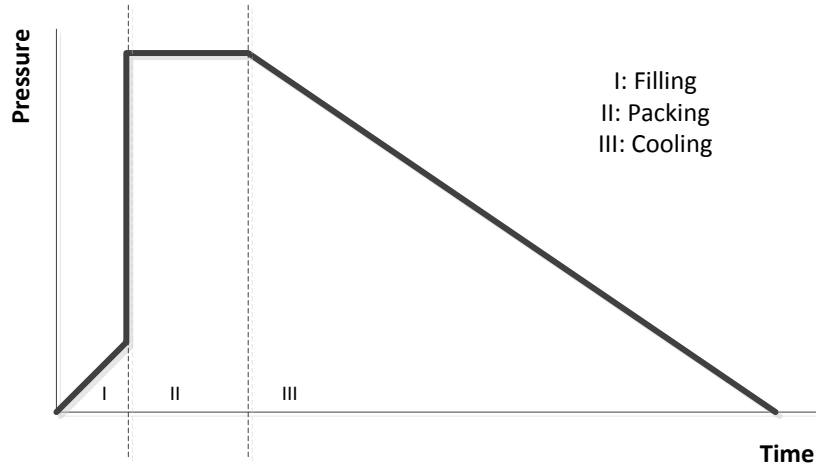


Figure 1-6 Pressure diagram of injection molding cycle

The packing stage of an injection molding cycle starts when the cavities are filled. At this stage, shear thinning behavior has no significant effect and the viscosity of the polymer depends only on temperature of the melt. When plastic cools and solidifies, it shrinks because of phase transformation from liquid to solid; and the distance between molecules is shortened. The loss of volume in the molded part can cause severely fault appearance issues and make the part not function as it is supposed to. So the purpose of the packing stage is to maintain pressure and push a compensation flow into a cavity to make up for lost volume from shrinkage until the gate freezes [4].

Creeping flow which compensates the lost volume would create core orientation. Therefore, increasing packing pressure and packing time to push more flow will also generate a larger level of molecular orientation in a molded part, particularly near the gate. In addition,

higher packing pressure and packing time can reduce melt relaxation, so that more flow-induced residual stress is retained [5].

For the reasons above, packing parameters, including packing pressure and packing time, greatly influence molecular orientation which seriously affects optical properties of clear polymers. So the target application of applying melt modulation technique to packing stage is optical product manufacturing. This research focuses on controlling packing parameters by using melt modulation system and investigates the effect of control valve on optical properties of molded plastic lens.

As will be presented in detail in the next chapter, many studies were conducted to investigate the effect of injection molding parameters, not only packing pressure and packing time, on the optical properties of clear polymer products. The results from those works clearly show that packing parameters are the main factor to determine optical quality in term of both precision of geometric dimension and birefringence. However, even though those results indicate that packing parameters obviously can control the optical quality, the experiments and simulations were done in case of single-cavity mold or identical multi-cavity mold. For a mold with a symmetric runner system and identical multi-cavities, packing parameters were equally applied to all cavities. This limitation cannot cope with the family molding purpose because different sizes and shapes cavities require different packing pattern.

Applying the melt modulation technique could overcome this limitation. By controlling packing parameters independently in each cavity, the required optical quality for each part could be achieved. From this motivation, the objectives of this thesis were identified as follow:

- **Investigate the effect of processing parameters on the optical quality of an injection molded product.**
- **Modify the previously developed melt modulation systems and mold for packing stage control purpose**
- **Investigate the capability of melt modulation systems to control a pressure profiles during the packing stage by numerical simulation.**

Starting from the original bulky design, Akapot Tantrapiwat developed the hardware of melt modulation system and the melt control methods [2] in order to enhance the polymer filling process. Since the previous melt modulation system and testing molds were mainly designed for improving filling pattern of polymer melt, the system could be modified to work better with packing stage control application. First a series of experiments and MoldFlow software simulations were conducted in order to investigate the effect of injection molding parameters on clear polymer products. Results from this part will be a solid reference showing that different parameters would definitely lead to different properties, including optical quality.

Next all the existing equipment was evaluated. A new mold was designed and built to enable the evaluation of optical properties. And the compact melt modulation hardware was modified to be simpler and work better with the new mold. All newly modified equipment was used to perform a set of experiments which corresponds to second and third objectives. Throughout this thesis, details of the idea, approach, design, and results are presented and written according to the thesis outline as follow.

1.3 Thesis Outline

The thesis presents research focusing on expanding the limitation of the melt modulation technique to the injection molding packing stage. It is composed of 6 chapters which include the current chapter as an introduction.

Chapter 2 explains the necessary scientific background related to the thesis. It also describes a basic theory regarding pressure drop through the melt delivery system and valve. The melt modulation system developed by Tantrapiwat is presented from hardware to melt control method, including significant results from this new model. In addition, the theory of polymer birefringence is also briefly explained. This chapter also includes the information about some quality parameters in plastic optics and some literature review showing how injection molding parameters influence those qualities. Chapter 2 is closed with the system's limitations and challenges which point to a goal to achieve.

Chapter 3 presents the first set of experiments and numerical simulations investigating the effect of packing parameters on both physical and optical properties of injection-molded products. The dog bone specimen was used as a sample for this chapter. The ideas, approach, and experimental setup are described in detail. Results from both experiments and numerical simulations show how much each parameter has influence to the properties.

Chapter 4 illustrates the equipment and machine used in this thesis, including mold base, pressure transducer, and injection molding machine. The newly-modified design of compact melt modulation system and mold for packing stage control purpose are also presented. It shows the concept, idea, design process, and details for each component utilized in the new application.

Chapter 5 presents the implementation of the new melt modulation system for packing stage control. A set of numerical simulations was performed by using 3D model of the mold and the valve designed in Chapter 4. The purpose of the simulation is to see the effect of the control valve on the pressure profile in the cold runner system designed in Chapter 4 also. This chapter also presents the experimental approach to investigate the capability of the system as a function of packing pressure, packing time, and valve angle in the future experiment.

The final chapter, Chapter 6, summarizes and concludes all of the work done throughout the thesis. It shows the impact of this research to the plastics industry. At last, recommended future works to continue the development of the melt modulation technique are summarized.

CHAPTER 2 – RELATED BACKGROUND

2.1 The Original Melt Modulation Technique

The melt modulation system was previously designed for the filling stage of injection molding processes. Instead of retooling the mold by changing the melt delivery system layout in order to control the amount of melt flow into different size and shape cavities, a mechanical control valve is placed at a specific location in the runner. The valve acts as a melt control device which restricts the amount of melt flow going through it by rotating to a specific angle, θ , relative to the runner. Figure 2-1 illustrates a diagram of applying such a control valve to the runner. At Lehigh University, the original design was adapted from common rotary plug valves and used with non-circular runners because of simplicity of mold machining and flexibility to change the valve position easily. So the melt modulation control valve looks like the bottom half of a regular rotary plug valve.

To control the melt flow, the valve is initially turned to a specific angle depending on the level of desired flow restriction, then the injection molding cycle starts normally. During the filling process, the molten polymer is injected from the sprue to the cavity by passing through both the runner and a valve port. For a cold runner system, the solidified runner has to be ejected with the part. An ejection problem usually occurs when the valve is set to a nearly closed position. At this instant, the solidified polymer breaks at the joints between the valve and the runner due to small cross-sectional area [2]. This leaves a solidified polymer piece stuck in a valve port. A small ejector pin is inserted at the valve center to solve this problem so that it could push the solidified polymer left in the valve port out. The sequence for a traditional method of melt flow control is illustrated in Figure 2-2.

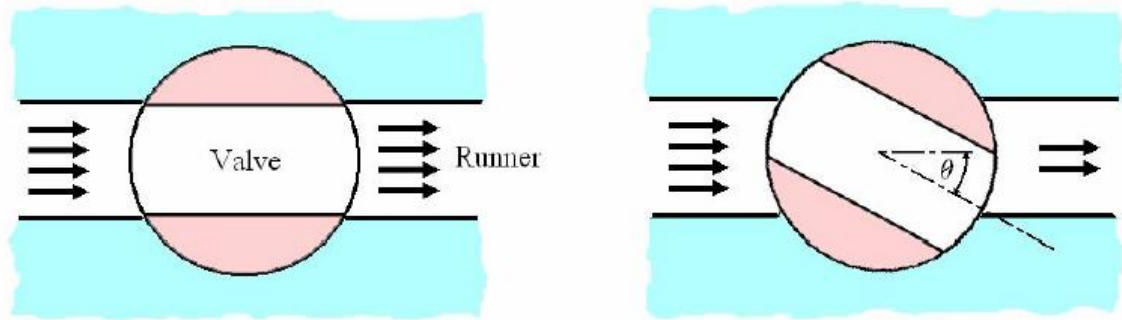


Figure 2-1 Rotary plug valve used with the runner [2]

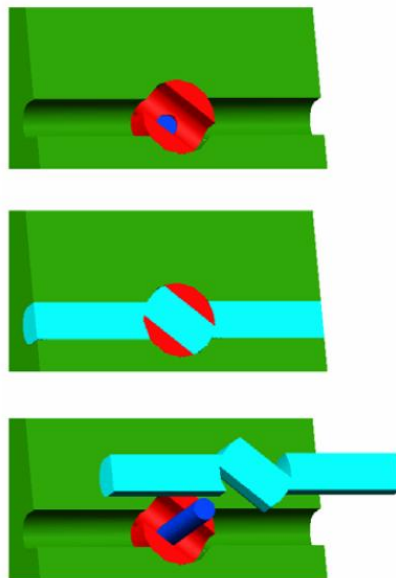


Figure 2-2 A traditional operation sequence of melt modulation system [2]

In addition to using a melt modulation system, there were attempts to control melt flow and pressure of the cavities to improve the process. Kazmer developed a dynamic valve system to use with multi-cavity molds for hot runner systems [6, 7]. The valves are independent of each other, and each valve is used to control one cavity by a rapid-response hydraulic actuator. Since the valve is able to be controlled in real time during the molding

cycle, the filling and packing stage control can be decoupled from each other, i.e. applying one flow rate profile and a completely different packing profile. Another approach to control the pressure in the mold cavity was developed by Harry [8]. By investigating the possibility of the pin used to monitor the resulting force from the molding cycle could act as a source of desired pressure. Generally, the pin is placed at the same level as the cavity surface, and the force acting on the pin is interpreted by load cells and associated equipment. Harry conducted the experiment by pushing the pin on the resin in the cavity to see its effect on packing profile. The last example case is balance filling of family molding. Park optimized the size of the runner for each cavity so that the different cavities would be filled properly [9]. The system he developed is called a Variable-runner system. Moreover, he investigated the effect from changing the runner size and processing conditions in terms of shear rate, and the viscous heating.

2.2 Control Valve Fundamentals

As the flow rate is a function of valve opening percentage, the ideal case for the relationship is a linear curve between flow rate and valve travel so that the designer can control the flow rate more precisely and easily. Unfortunately, most control valves cannot achieve that characteristic and may vary in different flow system because of valve port geometry and valve type [2]. Figure 2-3 presents the different inherent flow behavior resulted from different control valves.

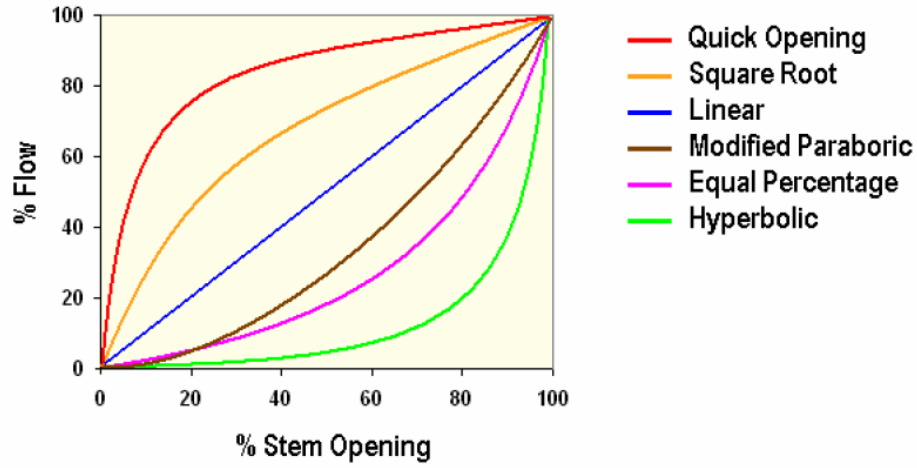


Figure 2-3 Range of inherent flow characteristics for different control valves [2]

In addition to valve performance itself, the mold configuration also has a great effect on actual flow performance of the entire system. The actual performance of the flow system can be defined from a reduced pressure ratio, P_R , as follow:

$$P_R = \frac{\Delta P_{valve}}{\Delta P_{system}} \quad (2-1)$$

with ΔP_{valve} and ΔP_{system} representing pressure drop across the valve and the entire mold system respectively.

As the reduced pressure ratio decreases, pressure drop across the valve has relatively low portion compared to pressure drop of overall system, and the inherent flow characteristic curve would be shifted toward the characteristic of a quick-opening type as presented in Figure 2-4. In order to achieve linear flow performance when this system is installed, an equal percentage type valve with an appropriate size should be selected.

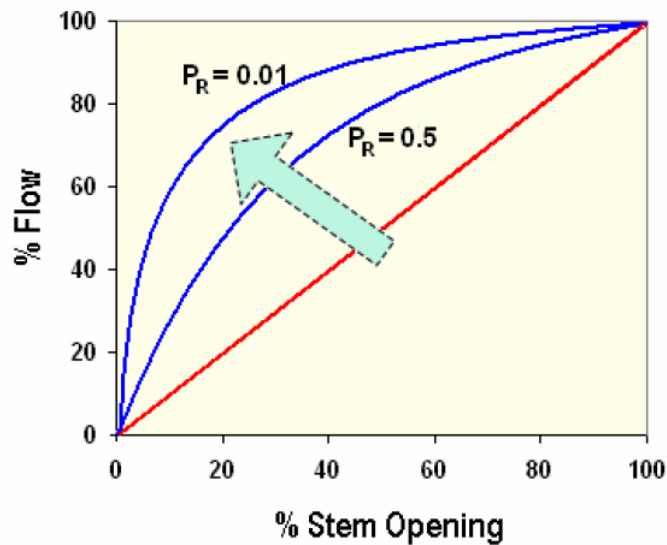


Figure 2-4 Shifting of flow behavior due to reduced pressure ratio [2]

The original melt modulation system was designed to work with two control valves. Both valves were located in the primary runner of a symmetric system at the same distance from the sprue. The traditional control method used for the original system consisted of leaving one valve at a specific angle, and controlling the other valve so that when polymer is injected into the family molding system, the amount of melt flow would go differently through both valves and fill different cavities properly. From Figure 2-5, by rotating Valve A toward a fully-closed position, during the filling stage, most of the melt flow tends to flow through Valve B which is left fully open. The experiments by Akapot Tantrapiwat [2] indicate that the melt flow difference through each valve versus the percentage of Valve A closing has a quick opening characteristic as shown in Figure 2-6. This behavior is obviously not a desired one compared to linear relationship.

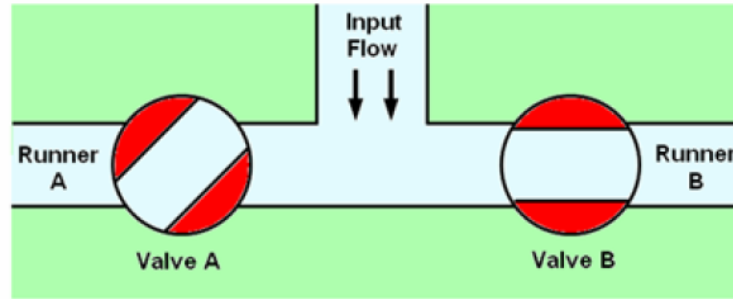


Figure 2-5 Traditional control method for two valves system [2]

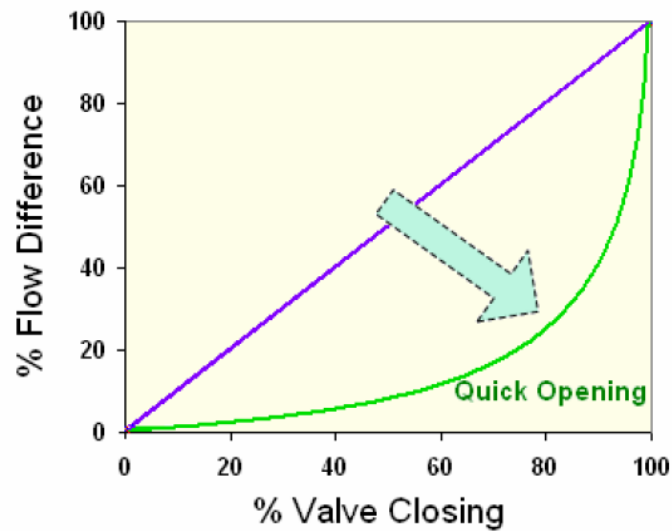


Figure 2-6 Flow behavior of original melt modulation system [2]

2.3 Pressure Drop in a Cold Runner System

In order to fill the polymer through the cold runner system, the injection pressure produced by the injection molding machine must be greater than the pressure drop of the entire system, including sprue, runner, valve, gate, and cavity. The pressure drop of the runner depends on a “shape factor”, ratio of the perimeter to the area of a runner’s cross-sectional shape as described in Figure 2-7. The red line represents the perimeter and the green

area represents cross-sectional area. The higher shape factor means the runner is less efficient and will cause more pressure drop per volume than the lesser value.



Figure 2-7 Shape factor

The runner shape which yields the best shape factor is the circular type. For the melt modulation technique, the full-round runner is not necessarily the best choice because the mold needs to be machined in both halves (half-circular shape per side) which requires a costly high precision operation. Then there is also a risk that both halves of the runner would not match perfectly to each other, and cause the system not to work as desired [1].

Alternatives to the circular runner have been designed in order to reduce the complexity of mold construction so that they require only one side of mold machining operation. According to the data from John Beaumont's Runner and Gating Design Handbook [1], the acceptable alternatives based on the full-round runner system are parabolic and trapezoidal, which are presented in Figure 2-8. Note that the recommended draft angle for parabolic and trapezoidal runner is 5° to 10° .

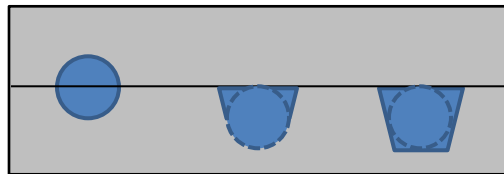


Figure 2-8 Full-round, parabolic, trapezoidal runner [1]

2.4 Compact Melt Modulation System

From the bulky and expensive original melt modulation system, the primary design purposes for the system are to reduce the size and cost, be directly embedded with the mold, and to increase the filling performance. The considered development topic includes control valve, driving mechanism, controller, and control technique.

2.4.1 Control Valve

The valve stems used in the compact system were the same as those used in the original design for evaluating flow characteristics. The standard rotary plug valve was chosen from considering design criteria consisting of flow characteristics, mechanical properties, and process performance as shown in Table 2-1. Then the valve was modified to have an open port in order to work with the cold runner system. The drawing of the prototype of the original valve stem is illustrated in Figure 2-9. The two sides of valve port were designed to be tapered to match the shape of the runner, and make it easy to eject the solidified polymer.

Flow Characteristics	Mechanical Properties	Process Performances
Flow Capacity	Size(Device)	Repeatability over time
Range ability	Size(Mech/Actuators)	Adjustment Force/Torque
Performance Characteristics	Complexity	Packing Pressure Survival
Pressure Drop	Service Needs	Runner Ejection
Cavitations	Useful Life	Friction/Wear Surf.
Turbulence	Impl.(manual)	Friction/Wear Mech.
Flow Symmetry	Impl. (automatic)	Adjustment Time
In-Serv. Force/Torque	Impl. (manuf. plants)	App. to Different Polymers
Temperature Compatibility	Suitability Across Products	Short Volume
Thermo-phys. Degradation	Cost	
Inclusion Degradation		
Repeatability		
Leakage		

Table 2-1 Design parameters for valve selection [2]

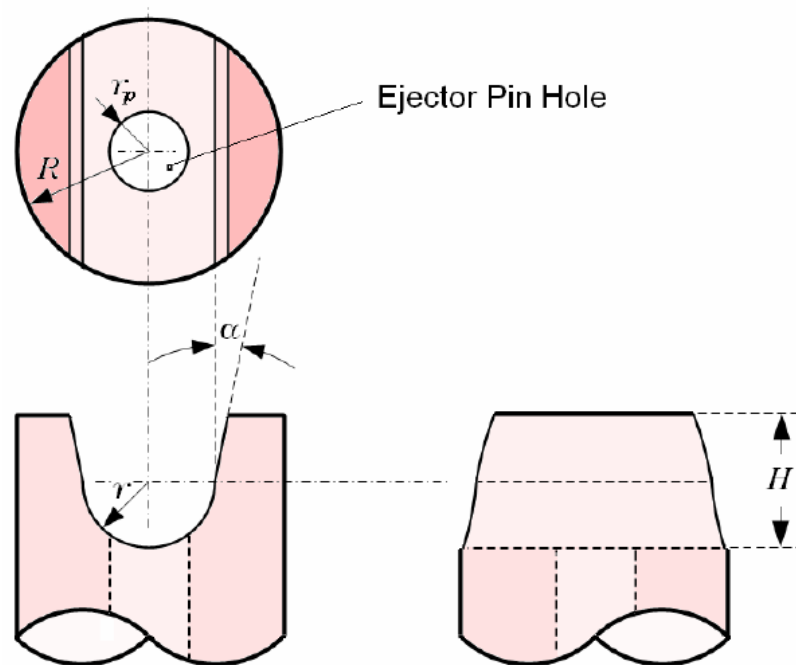


Figure 2-9 Original valve stem design [2]

From Figure 2-9, the original valve stem was designed to match the 0.0625 inch, r , parabolic runner. Therefore its diameter is 0.125 inch with a 3 degree of release angle, α . Even though there are three sizes of valve ports when the system was first developed (including the special V-shape characterized valve port which was developed later for an improvement of flow characteristic), only the smallest and biggest valve ports, which are 65% reduced port and full port, were used by Tantrapiwat to test the flow behavior with the compact system [2]. The information of the original valve stem is presented in Table 2-2

Valve	r (inch)	H (inch)	Max θ (degree)
Full Port	0.0625	0.125	60
80% Reduced Port	0.056	0.112	56.6
65% Reduced Port	0.05	0.100	53.6

Table 2-2 Original valve stem information

Because of the restriction of material removal described in Section 2-1, a 3/32 diameter ejector pin is inserted in the middle of a valve port in order to push solidified polymer out. Figure 2-10 shows the real original valve stem with an ejector pin.



Figure 2-10 Actual valve stem with ejector pin [2]

2.4.2 Driving Mechanism

A stepper motor was selected as an actuator for the compact system. The major concern of selection is the actuator has to be inexpensive and small enough so that it could be embedded at the back of the mold, but still generate high enough torque to drive a valve under high pressure conditions. To meet all the requirements, Tantrapiwat chose to use an RC servo which is used in radio control models.

A HITEC-5990TG model actuator was selected for the compact system. It can rotate from 0° to 180° maximum. The actuator is designed for a heavy duty by using durable titanium alloy gears with dual ball bearing, and ultra hardness shaft with three axial metal bushing. The package is tightly sealed to prevent water and dust [10]. All the components of the actuator are presented in Figure 2-11. The actuator works by receiving the input digital signal from controller to drive a high power DC motor to a desired position. Then the power is transmitted through a gear train to reduce speed and increase the torque of the output shaft. The output shaft is connected to a positioning sensor called potentiometer. The technical information of this actuator model is presented in Table 2-3.

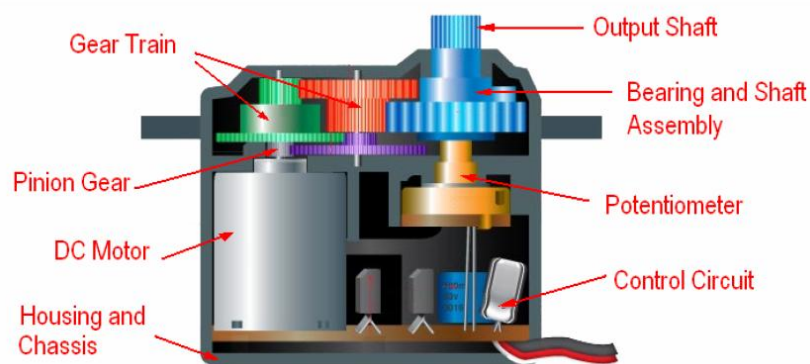


Figure 2-11 Actuator used in compact melt modulation system [2]

Specification	Values	Units/Description
Operating Voltage Range	7.4	Volts
Operating Speed	72	RPM at No Load
Stall Torque	2.94	N-m
Standing Torque	3.82	N-m
Idle Current	10	mA at Stopped
Running Current	380	mA at No Load Running
Dead Band Width	2	uSec
Operating Travel	90±1°	One Side plus Traveling
Dimension	40×20×37	Millimeter
Weight	68	Gram

Table 2-3 Technical data of compact melt modulation system actuator [2]

In the original design, the cable and pulley which were connected to a timing belt and actuator on the top of the mold were used to drive a valve. This system generated much additional friction that made it difficult to rotate the valve. By using the actuator selected above, the system is much smaller and could be embedded inside the mold. Since the original valve stem needs an ejector pin inserted in the middle of the valve port, the valve stem could not be directly coupled with the output shaft of the actuator. Hence the transmission system is required between the output shaft and the valve stem in the radius direction.

Two spur gears were selected for the single step transmission with 0.6 speed reduced ratio in order to increase the output torque. Spur gear transmission could reduce additional friction caused by the original design because typical gear train has high efficiency and small backlash. The specification of selected gears is shown in Table 2-4. The gear with 40 teeth is attached to the valve stem. On the other hand, the pinion with 24 teeth is connected to the output shaft of the actuator interposed by an insulator washer to prevent conducting heat from the pinion to the actuator. A prototype of the compact melt modulation system designed by Tantrapiwat is presented in Figure 2-12.

Specifications	Gear	Pinion
Pitch Number	32	32
Number of Teeth	40	24
Pitch Diameter	1.25 inch	0.75 inch
Outside Diameter	1.30 inch	0.8 inch
Pressure Angle	14.5 degree	14.5 degree

Table 2-4 Specification of gear mechanism for compact melt modulation design

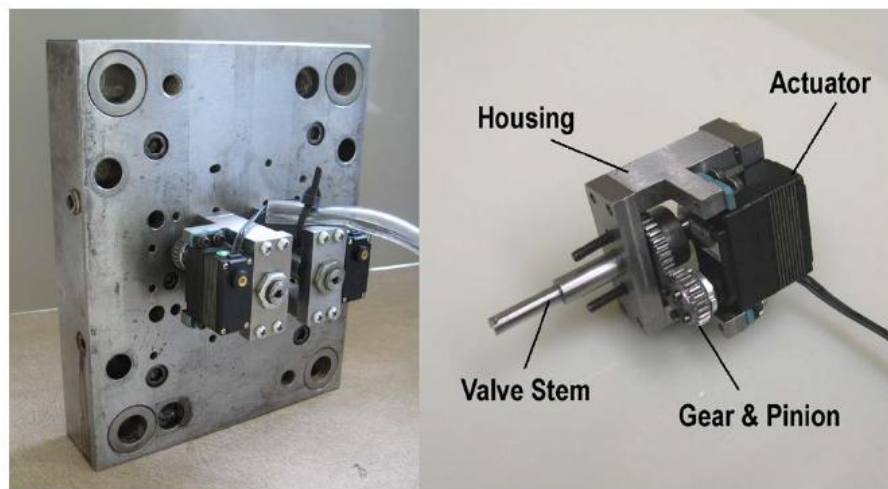


Figure 2-12 A prototype of compact melt modulation valve driving unit [2]

2.4.3 Controller

The new controller was designed by Tantrapiwat [2] during his Ph.D. study. It can operate individually and interface via a Universal Serial Bus (USB). Since the HITEC actuator has a potentiometer connected to the output shaft, it can be controlled by a normal 8-bit microcontroller with PD (proportional derivative) type control. This device performs a feedback control with the controller to compare the output variable (actual valve angle) with

an input parameter (desired valve angle), and any different between the two is used to drive the output into agreement with the input as shown in a diagram of Figure 2-13.

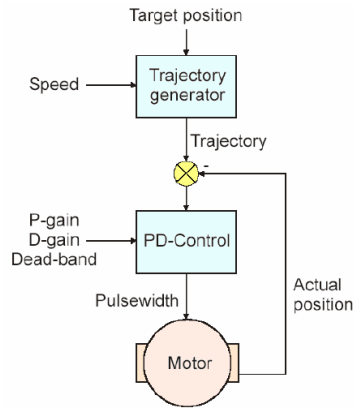


Figure 2-13 PD control diagram for the actuator [2]

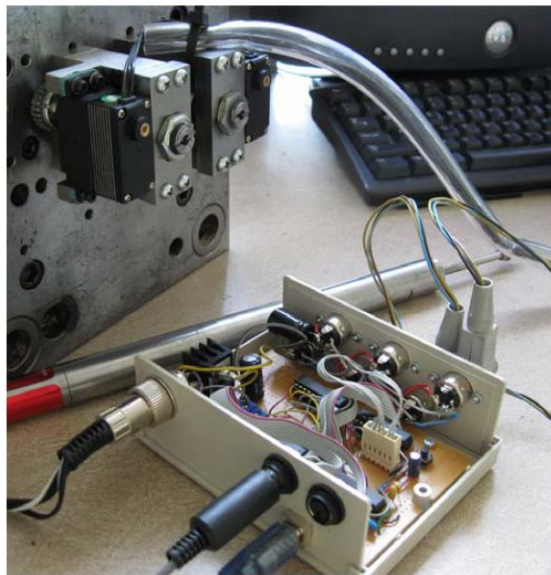


Figure 2-14 USB controller for the compact melt modulation system [2]

The compact system controller has a capability to control six individual valves. It continuously sends a pulse code signal to drive an actuator. In addition, it can read the injection screw ram position data from an Analog-to-Digital (A/D) converter so that it could

rotate valve angles as a function of ram traveling distance. Figure 2-14 shows a picture of the USB controller for the compact melt modulation system.

2.4.4 Control Technique

From the ability to read the injection screw ram position data from an Analog-to-Digital (A/D) converter of the new USB controller, the melt control method was improved far better than the traditional fixed-angle method. By introducing a position sensor called a LVDT (Linear Variable Displacement Transducer), the actuator could rotate valve angle as a function of ram traveling distance. Figure 2-15 illustrates the using of LVDT with injection molding system.

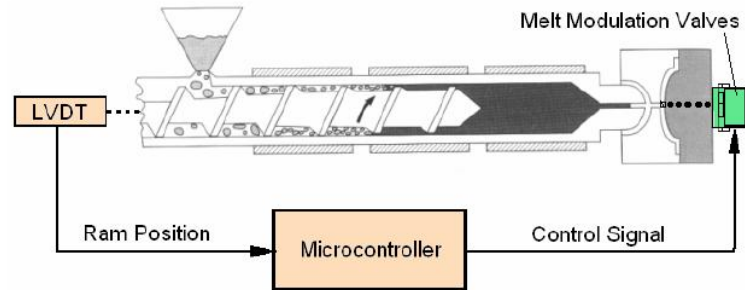


Figure 2-15 A control diagram with LVDT [2]

With this advantage, the actuator can drive a control valve to one angle before the injection cycle begins, and when the injection screw pushes melt flow and reaches an end position, the valve can be set to rotate back to fully-open position to avoid weak spots of solidified polymer between the valve and the runner. The new valve return cycle is shown in Figure 2-16. Then the driving mechanism design can be changed by removing a spur gear transmission. The valve stem can be connected to the HITEC actuator directly without ejector

pin in the middle of valve port. This advantage results in cheaper cost, less space required, and simpler construction.

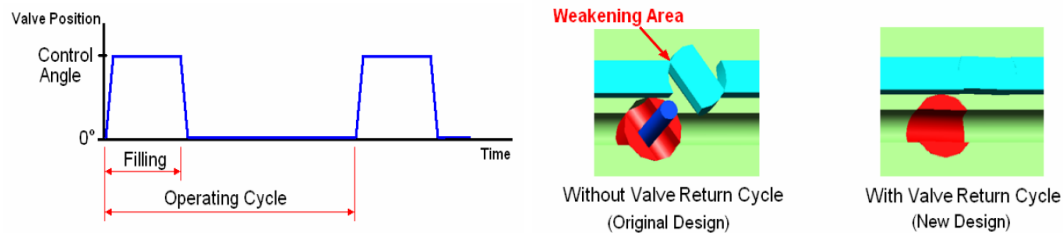


Figure 2-16 Valve return cycle for fixed-angle control method [2]

Even though the valve return cycle can solve the weak spot issue, the melt flow still possesses the quick-opening characteristic. In addition to the valve return cycle, Tantrapiwat developed two other control techniques which change the valve angle as a function of injection ram position. The new two control techniques are called Bang-Bang and Hybrid which provide better flow characteristics of polymer melt.

The **Bang-Bang** method controls the valve by only two positions, fully-closed and fully-open. The step function is used to determine the position of the control valve depending on an injection ram position. The diagram in Figure 2-17 explains the Bang-Bang technique. Although there is a delay from the time between a signal is input until the valve responds, it is not taken into consideration since this delay time is generally very short. The amount of melt flow through each valve is determined based on the needed volume of material for each cavity at the end of the runner.

The advantages of the Bang-Bang method over traditional fixed-angle method include simpler valve manipulation and less material damage from shearing. Because this technique requires only fully-closed and fully-open position, the control function could be

simplified. In addition, it can accept little error of valve angle. At the fully-closed position, the control valve can be rotated for a range to make sure that the runner is really shut-off. For fully-open position, a slight deviation of angle from the desired position does not cause the melt flow to change significantly due to quick opening characteristic. Moreover, the actuator can be changed to be simpler, such as a pneumatic cylinder or an electrical solenoid. From a material standpoint, since the melt flow does not have to flow through a narrow channel like in the fixed-angle method which generates high shear rate, the molded part has higher quality, especially higher strength.

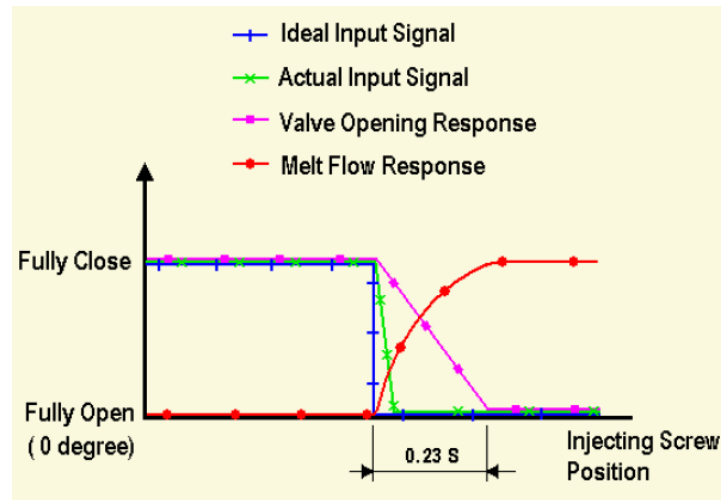


Figure 2-17 A timing diagram of Bang-Bang control method [2]

The limitation of the Bang-Bang method is when applying to a process which uses a small shot size and fast injection speed, it is difficult to control a valve properly. When the filling process starts, a control valve is set to be fully-closed and rotates to fully-open at a specified injection ram position. Before the control valve opens, the melt flow is stopped and can solidify. As a result, the solidified runner can prevent the cavity to be filled completely.

The **Hybrid** method is a combination between Bang-Bang and traditional fixed-angle method. Because of the concern that the melt flow will solidify when it stops in the Bang-Bang method, instead of shutting the runner off completely, the control valve is initially turned to a small fixed angle which could allow some melt flow to flow through it. Then at specified injection ram position, the control valve will be rotated to a fully-open position as same as Bang-Bang method. The timing diagram of Hybrid method is shown in Figure 2-18.

The downside of Hybrid is the same as fixed-angle method. When the melt flows through a narrow channel, it suffers from high shear rate which may degrade the quality of the molded part. Therefore the possible largest initial fixed angle is recommended and can be estimated about the one that allows the melt flow to fill 50%-80% of the runner across that valve [2].

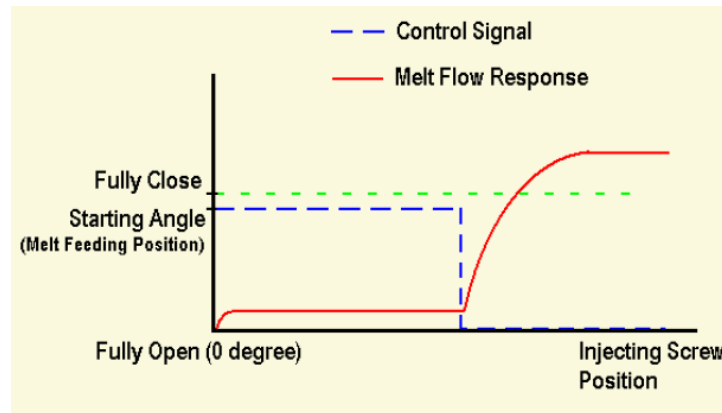


Figure 2-18 A timing diagram of Hybrid control method [2]

2.4.5 Flow Characteristic Results and Discussion

The experiment to evaluate the performance of the compact system with original valve stems was set up by using a BOY 15S injection machine with maximum clamping force

of 15 ton, and a shot size of 2.2 in³. The compact system is embedded to a DME A-series mold base size 9-7/8" x 8" [11].

The spiral-shaped cavity was designed to observe the flow length. The detailed dimensions are presented in Figure 2-19. Two identical spiral cavities were attached to the mold socket on the upper and lower side, symmetrically connected each other with non-circular runner described in section 2.4.1. The layout is shown in Figure 2-20. According to the figure, two compact melt modulation systems were used with two control valves. Valve A was connected to the upper cavity while Valve B was connected to the lower.

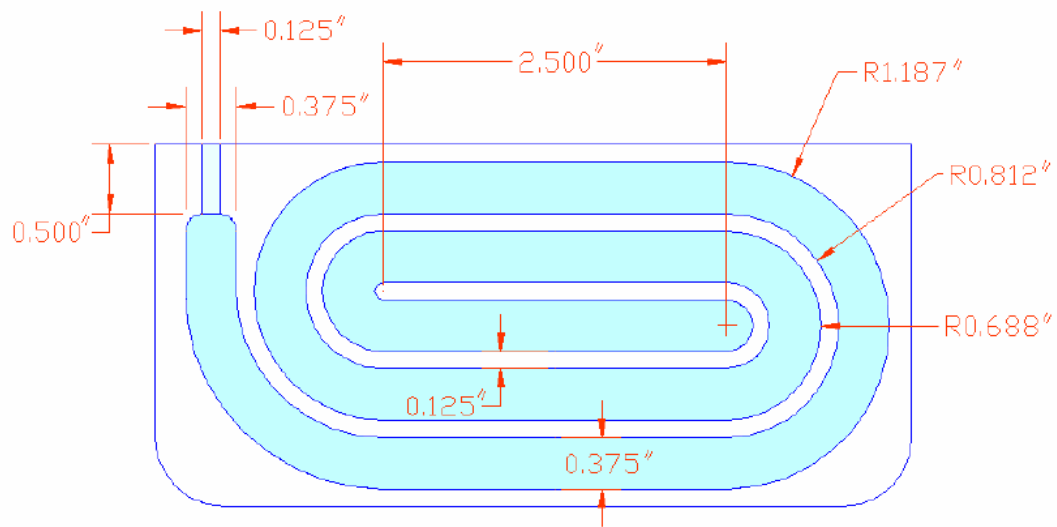


Figure 2-19 Spiral cavity drawing for the compact melt modulation evaluation [2]

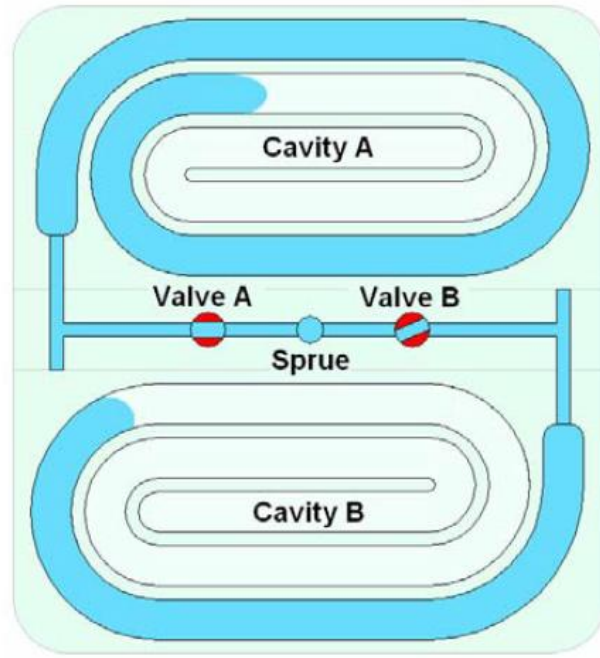


Figure 2-20 Spiral cavities layout [2]

By fixing Valve A to a fully-open position, the experiment was conducted by rotating Valve B at different angles to cause the amount of melt flow fills differently between the upper and lower cavity. Then the different flow lengths should be observed and calculated by:

$$\Delta_{flow} = \left[1 - \frac{FL_A}{FL_B} \right] \times 100\% \quad (2-2)$$

Where FL_A and FL_B are the melt flow length in Cavity A and B respectively. The original valve stems selected for this experiment are the full port and 65% reduced port as explained in Table 2-2. The tune range, 60 degrees for the full port and 53.6 degrees for the 65% reduced port, was divided into seven points equally from fully closed to fully open position.

The first experiment was done by using the traditional fixed-angle method. By tuning Valve B into different angles before the cycle begins. The result of different flow length is presented in Figure 2-21.

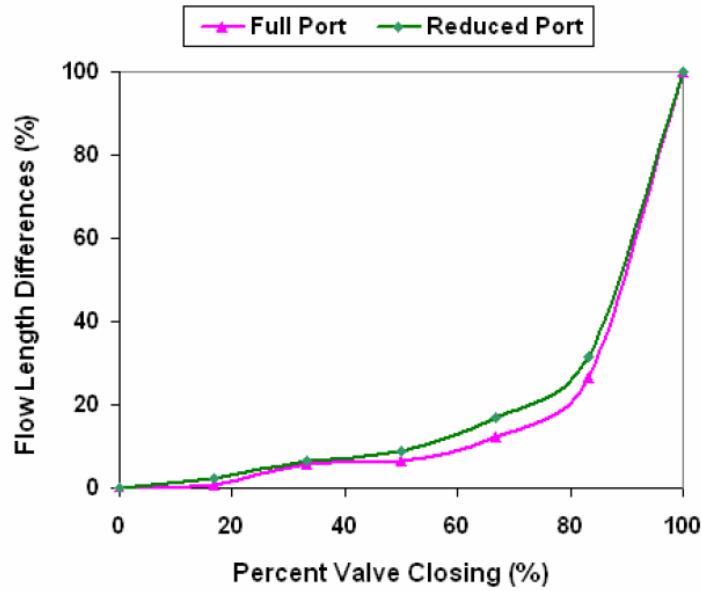


Figure 2-21 Valve characteristics using full port and 65% reduced port [2]

According to the result, the 65% reduced port could perform slightly closer to linear response due to the change of cross-sectional area between the runner and valve port. However, both results from the full port and 65% reduced port still possess a quick opening behavior which leads to difficulty to control the flow rate, especially at nearly close position.

Later, the Bang-Bang and Hybrid methods were applied to evaluate the different melt flow lengths. The experiment was basically set up as the same way in fixed-angle method. Adding another important parameter, the volume of polymer injected prior to the time of valve opening, varied from 0 to 2.2 in³ 10 steps equally. The initial fixed angle for Hybrid method was set to 3 degrees for the full port, and 2.5 degrees for the 65% reduced port. The flow length different result from Bang-Bang and Hybrid method with different valve port is presented in Figure 2-22, and the comparison between all three methods is shown in Figure 2-23.

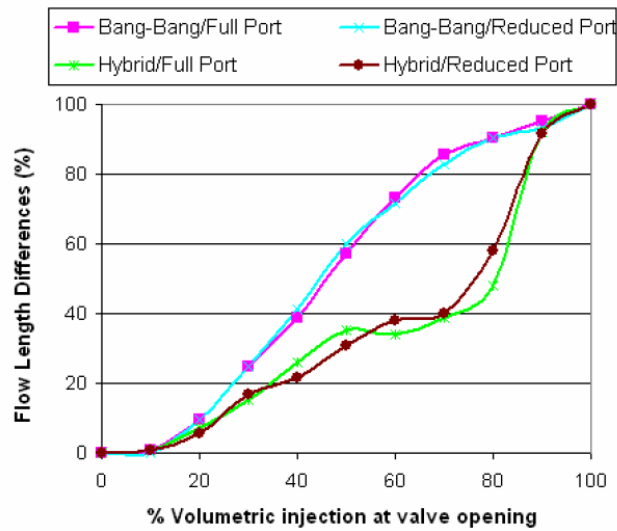


Figure 2-22 Flow characteristic of Bang-Bang and Hybrid method from different valve port [2]

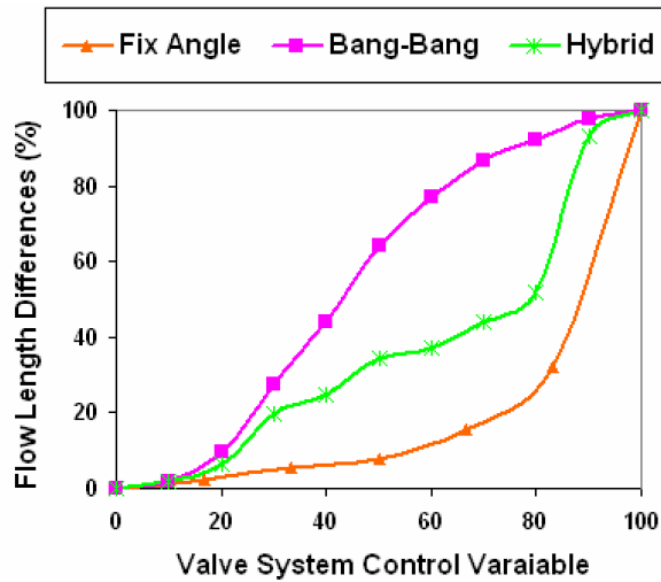


Figure 2-23 A comparison between three control methods [2]

The results show that using the developed control techniques, Bang-Bang and Hybrid, provides a dramatic improvement of flow behavior to become more linear response. And using a different control technique can produce a much larger effect than different valve ports.

2.5 Polymer Birefringence

Birefringence in a molding is an important property of optical parts. It is widely used to determine molecular orientation in transparent parts because of its simplicity of measurement [12]. Birefringence is mainly caused by flow-induced residual stress [13] and can be seen by passing polarized light through the stressed transparent material which has two refractive indexes. The refractive index, n , is defined as a ratio of the speed of light through vacuum (3×10^8 m/s), c , by the speed of light through the material, v .

$$n = \frac{c}{v} \quad (2-3)$$

Normally light moves through a transparent material in form of waves which are omnidirectional. By passing the light across a polarizing lens, called a polarizer, there is only one light wave component allowed to pass. When the polarized light passes through the transparent material, it is separated into two wave fronts which have different velocities. Each wave front is parallel to the direction of principal stress, σ_1 and σ_2 , of that material piece. In order to observe birefringence, another polarizing lens called an analyzer needs to be placed in the path of polarized light from the material. The analyzer can be rotated in order to control the light intensity that will pass through. Finally, the two wave fronts will interfere to each other which results in noticeable color spectrum. The schematic diagram showing how to observe birefringence is presented in Figure 2-24.

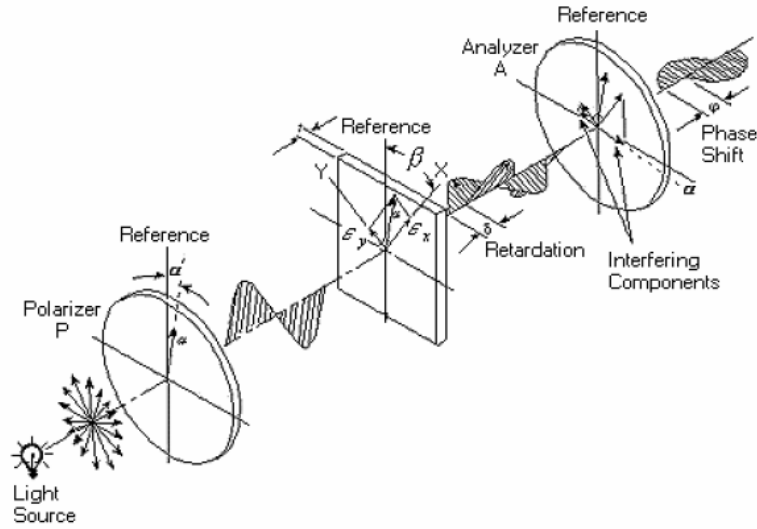


Figure 2-24 Schematic of plane polarize scope activity [8]

Birefringence can be determined as the difference of two refractive indices in the material which is directly related to the stress applied. The relationship is called Brewster's Law:

$$\Delta n = n_1 - n_2 = C(\sigma_1 - \sigma_2) \quad (2-4)$$

Where C is the photoelastic coefficient depending on type of polymer. Some values of C for optical polymers are shown in Table 2-5. According to the equation, high molecular orientation results in more difference of principal stresses, which will generate high birefringence consequently.

Since birefringence cannot be directly calculated by observing a polarizer, retardation, δ , is introduced. Retardation is the phase difference between two wave fronts which travel through the material. It controls the intensity of the color spectrum displayed by a polarizer. The relationship between retardation and birefringence is determined by the following equation.

$$\Delta n = \frac{\delta}{t} \quad (2-5)$$

Where t is a thickness of the material used to observe birefringence. Retardation value can be calculated by the relationship between the wavelength (λ) passed the selected band pass filter and the fringe order (m) which can be manually counted through polarizer.

$$\delta = m\lambda \quad (2-6)$$

Polymer	Photoelastic Coefficient, C ($\times 10^{-13} \text{ cm}^2/\text{dyn}$)
PMMA	-6
PC	72
COP (Zeonex 480R)	6.5
PS	-55

Table 2-5 Photoelastic coefficient of polymer [9]

Birefringence can be considered as a disadvantage for polymer optical products because it makes the images of object difficult to be accurately focused around the focal area [13].

2.6 Plastic Optics Quality

Optical devices are important equipment which performs optical transmission, recording, replay, or display. Transparent polymers which possess good optical properties have generally been used to manufacture plastic optics. The most widely used polymers in this industry are polymethyl methacrylate (PMMA), and polycarbonate (PC) because of their excellent transparency [13]. In many applications, designers mostly choose plastic optics over

glass due to its attractive advantages, such as lighter weight, lower cost, and higher impact resistance. In addition, it provides more configuration possibilities by using aspherical lenses which simplify the design, reduce part number, weight, and cost also. Moreover, compared to hi-grade glass materials, plastic optics has the same level of light transmittance. When plastic piece breaks, the scraps are larger and more obtuse, so it is less dangerous compared to glass.

Glass materials have more variety and could overcome plastic when high reliable and stability are needed. Plastic optics has lower temperature resistance and could only operate under certain thermal limit depending on each polymer. By the way, glass optics are not suitable for mass production. Instead of grinding and polishing each complex-shaped glass aspherical lens, the mold cavity can be machined into the desired shape only one time and used it in injection molding process to increase productivity [14].

The main factors which seriously affect the quality of plastic optics can be classified into 2 categories. The first is the factors which generate birefringence in material and another is the ones that cause the geometric dimension changes from the desired shape.

The two mechanisms which cause birefringence in the material during injection molding process are flow-induced and thermal-induced residual stress. Flow-induced residual stress is resulted from the frozen polymer chain orientation during filling and packing stage, and its incomplete relaxation during cooling stage [15, 16]. Pantani from University of Salerno investigated the effect of packing pressure on the morphology evolution and showed that more packing pressure can make the polymer has more molecular orientation [17], which retains flow-induced residual stress in the part [5]. Then more birefringence can be observed. Li from ZhengZhou University conducted the experiment to investigate the effect of injection molding parameters on optical properties of rectangular plate polystyrene [18]. The results clearly show that increasing packing pressure produces more fringe number and haze, which

are poor characteristics of optical products. On the other hand, thermal-induced residual stress results from unbalance cooling of the part. Although flow-induced residual stress is relatively small compared to thermal-induced residual stress, but it is the main part that creates birefringence. Pai and Huai from National Tsing Hua University measured the proportion of birefringence which results from two types of stresses. As a result, flow-induced residual stress was found to be more effective at about 92% [15].

Geometric dimension tolerance is another crucial factor that defines the optical quality. For example, a poor-shaped lens could have a wrong focal point and cause optic aberrations in object images. Major dimensional errors that could occur in injection molded optics are shrinkage, warpage, and surface quality. The shape quality of molded optics mostly depends on processing parameters of injection molding process, including melt temperature, mold temperature, packing pressure, and packing time. However, the shrinkage behavior also results from flow-induced residual stress in the direction perpendicular and parallel to the melt flow [16]. Hu conducted research with PMMA aspherical lens parts manufactured with different condition of packing parameters [19]. The experiment result shows that when packing time is enough, packing pressure not only determines the part shrinkage size but also affects its uniformity. In contrast, even though increasing packing parameters could reduce shrinkage behavior, it will cause more amount of warpage [20]. In the aspect of surface quality, the experiment done by Tsai presents the result from processing parameters to surface quality of lens, such as light transmission, surface waviness, and surface finish. As expected, increasing packing pressure greatly improves the surface waviness of the tested lens. Conversely, all processing parameters have only little effect on light transmission and surface finish of lenses [21].

2.7 Limitation and Challenges

Since its first invention, the melt modulation technique has been developed for years at Lehigh University. It continues to show how its capability makes a contribution to an injection molding industry. From the original bulky and impractical design, a series of experiment and analysis was done by Layser to understand its characteristic and to utilize it more widely, such as weld-line positioning technique [3].

Tantrapiwat came after that to continue improving melt modulation technique in the same research group at Lehigh University. He designed the overall system to be simpler, less expensive, and higher efficiency to suit the actual industrial application. From only two valves application, four valves were successfully used in his research. Moreover, the traditional fixed-angle control method which yields undesired quick-opening flow behavior was improved. Bang-Bang and Hybrid control method based on injection ram position shows greatly improvement of flow characteristic toward linear respond [2].

Even though the past results would show that melt modulation technique does benefit an injection molding process, it is restricted to be utilized only during filling stage in spite of the fact that a control valve affects the pressure in the cold runner system. Since packing parameters seriously affect the quality of plastic optics in terms of birefringence and dimension tolerance, lens-shaped parts are chosen for this research. Although there are many researchers trying to investigate the effect of process parameter on optical quality, the conventional injection molding could not fully modify the optical properties of plastic lens to be different in each cavity due to the uniform packing parameters through the entire cold-runner system. The challenge of this research is to expand the capability of melt modulation technique to the packing stage by controlling packing parameters, including packing pressure

and packing time, in order to mold lenses which have the desired and different optical properties in one cycle.

CHAPTER 3 – The Effect of Processing Parameters on the Properties of Injection-Molded Product

3.1 Introduction

This chapter presents a series of numerical simulations and experiments to study the effect of processing parameters on the properties of injection-molded test specimens. The results from this chapter would provide a solid reference when applying melt modulation systems later. In the work Chapter 3 is divided into two main parts. The first part is the numerical simulation using MOLDFLOW software to investigate the quality of the molded part in terms of geometric dimension tolerance, while the second part is an experiment to show variation of the optical quality and strength due to different processing conditions. The part used to investigate properties in this chapter is a dog bone shaped standard tensile test specimen (ASTM D638 – Type I). The geometry and dimensions of a dog bone cavity is presented in Figure 3-1. The dog bone cavity was presented in the ASTM standard mold which was used throughout the study. The mold layout is shown in Figure 3-2. The injection molding machine used to conduct the experiment was a Nissei model PS40E5ASE (Figure 3-3) for which some specifications related to its injection unit are presented in Table 3-1.

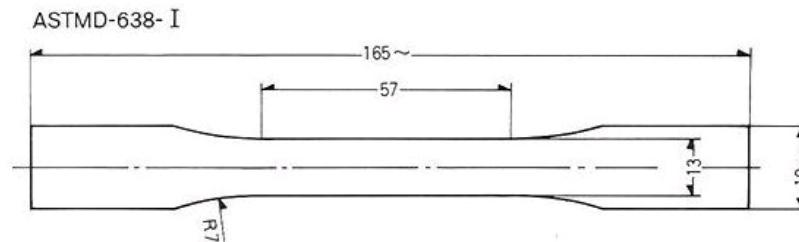


Figure 3-1 ASTM - D638 Type I dimension in millimeter [22]

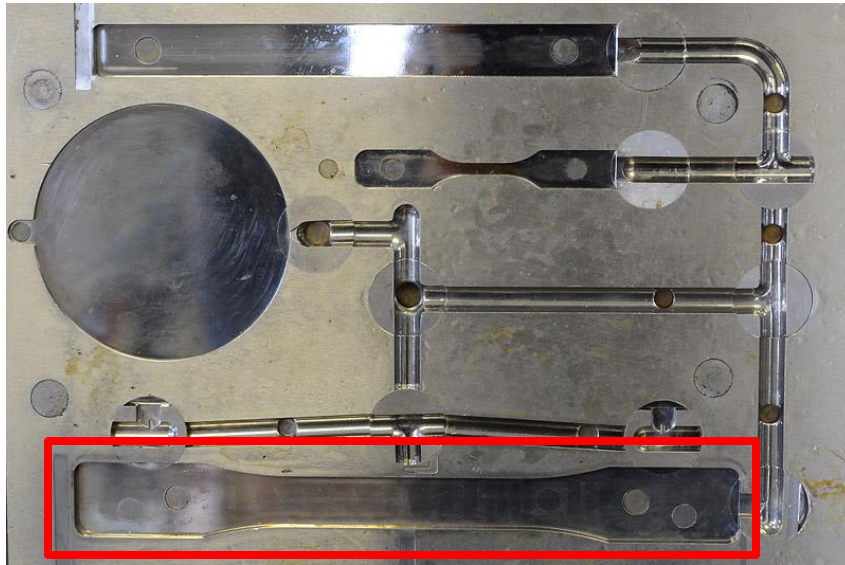


Figure 3-2 ASTM mold cavities



Figure 3-3 Nissei machine model PS40E5ASE

Specification (unit)	Values	Specification (unit)	Values
Screw Diameter (mm)	26	Injection Rate (cm ³ /sec)	71
Injection Capacity (cm ³ /shot)	49	Screw Stroke (mm)	92
Plasticizing Rate (kg/hr) - PS	22	Screw Speeds (rpm)	0-335
Injection Pressure (kg/cm ²)	1870	Clamp Force (ton)	40

Table 3-6 Injection unit specifications of Nissei machine [23]

3.2 Numerical Simulation

The objective of this series of numerical simulations was to investigate the effect of processing parameters on weight and geometric dimensional quality, including shrinkage, and deflection. A 3D model of a dog bone specimen was created as well as the cold runner system corresponding to the actual ASTM standard mold, and then imported to Moldflow software.

The dog bone shaped model was meshed using a 3D approach which fills the volume of the model with four-node, tetrahedral elements [24]. The 3D mesh is suitable for a thick, solid part because it gives a true 3D representation of the imported model. The total meshed tetras in the model were 5,245 elements connected by 1,029 nodes. The cold runner system and the sprue were duplicated from the actual mold in Figure 3-2. The 39 elements of 1D beam were used to model them by default. The total volume of the dog bone cavity and the cold runner system, including the sprue, were 8.1427 cm³ and 8.8439 cm³ respectively. Figure 3-4 presents the 3D meshed model of the dog bone specimen and the cold runner system used for numerical simulation.

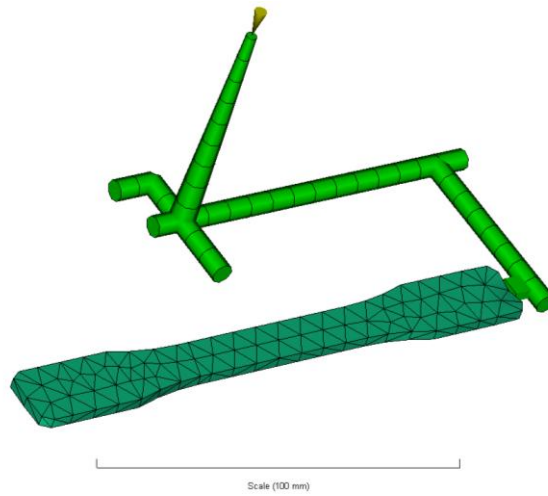


Figure 3-4 3D meshed model in MOLDFLOW

Three common optical polymers were chosen for the numerical simulation; polymethyl methacrylate (PMMA), polycarbonate (PC), and polystyrene (PS). To analyze the effect of each parameter, a Taguchi method with a $L9(3^4)$ orthogonal array was used to conduct the simulation by setting four parameters to have three levels each. Table 3-2 shows all levels of each parameter selected for the $L9$ array in Table 3-3.

Material	Parameter	Symbol	Level 1	Level 2	Level 3
PMMA	Mold Temperature (C)	A	38	58	80
	Melt Temperature (C)	B	240	260	280
	Packing Pressure (MPa)	C	30	75	120
	Packing Time (s)	D	2	8	15
PC	Mold Temperature (C)	A	80	91	102
	Melt Temperature (C)	B	286	296	324
	Packing Pressure (MPa)	C	30	75	120
	Packing Time (s)	D	2	8	15
PS	Mold Temperature (C)	A	30	45	60
	Melt Temperature (C)	B	198	219	240
	Packing Pressure (MPa)	C	30	75	120
	Packing Time (s)	D	2	8	15

Table 3-7 Parameters used for numerical simulation

3.2.1 Average Volumetric Shrinkage

According to the MOLDFLOW manual [24], the average volumetric shrinkage result shows the average value of volumetric shrinkage over the half-gap thickness of the 3D model, as a percentage of the original volume. Volumetric shrinkage is the increasing percentage of local density from the time packing stage ends until the part cools down to the ambient reference temperature. High volumetric shrinkage results in sink marks and voids in the molded part. Moreover, non-uniform volumetric shrinkage may cause the part to warp at the end. From numerical simulation, the Taguchi results of average volumetric shrinkage for PMMA, PC, and PS are presented in Figures 3-6, 3-7, and 3-8 respectively.

PMMA

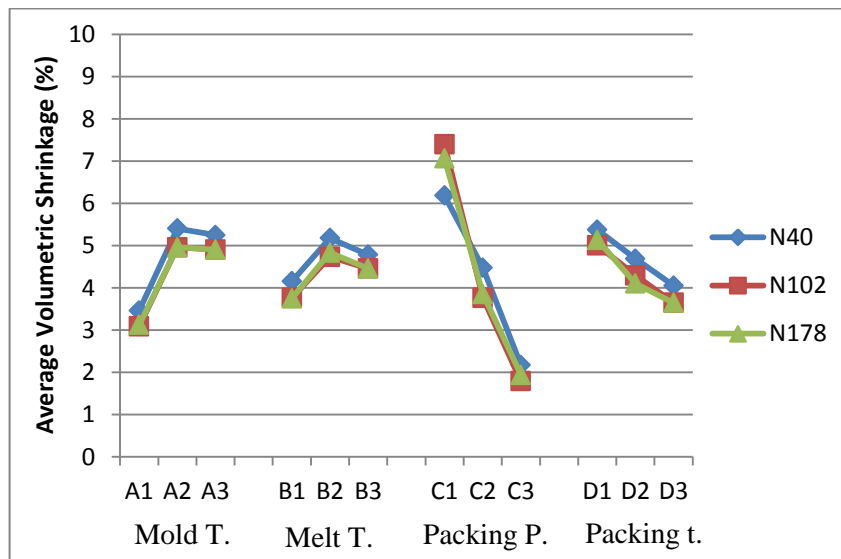


Figure 3-6 Average volumetric shrinkage result for PMMA dog bone (Numerical)

PC

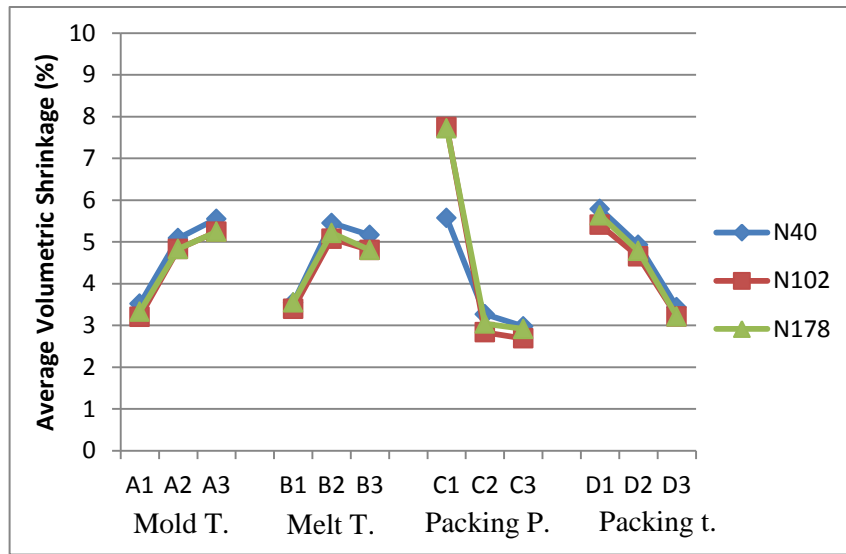


Figure 3-7 Average volumetric shrinkage result for PC dog bone (Numerical)

PS

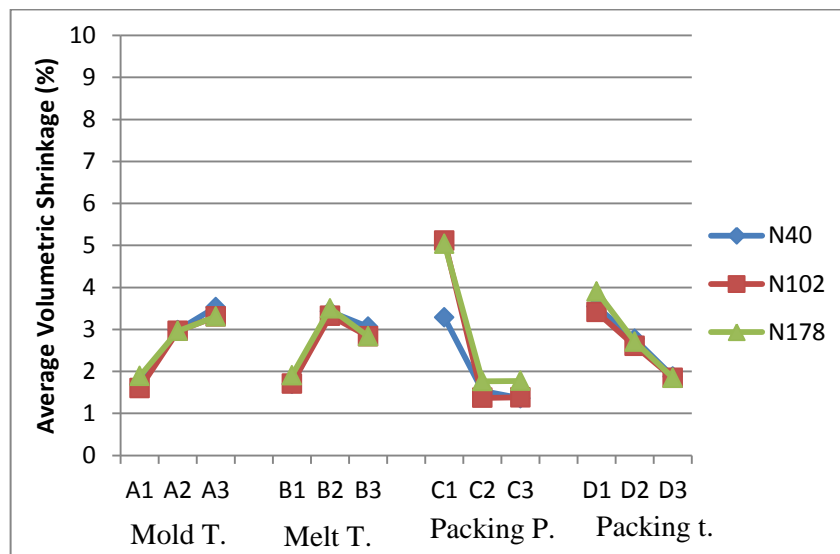


Figure 3-8 Average volumetric shrinkage result for PS dog bone (Numerical)

3.2.2 Deflection

An overall deflection result can be represented as the total warpage that occurred from all contributors in each node. Practically, it is determined by the stiffness of the part and the level of non-uniform shrinkage. If the part is stiff enough to not allow deflection to occur, residual stresses can be created during a process [24]. There are many causes of warpage, but they can broadly be classified as the one due to non-uniform shrinkage, and due to unbalanced cooling [4, 20]. The warpage due to non-uniform shrinkage is smaller when compared to the unbalanced cooling cause. Increasing of packing parameters, packing pressure and packing time can reduce the non-uniform shrinkage, however, the unbalanced cooling warpage becomes worse [20]. In the numerical simulation, the mold temperature was set at constant temperature with no cooling line inside. Therefore, it can be assumed that the cooling rate in all simulation results is constant throughout the part, and there is no deflection from unbalanced cooling. From numerical simulation, the Taguchi results of total deflection in all directions for PMMA, PC, and PS are presented in Figures 3-9, 3-10, and 3-11 respectively.

PMMA

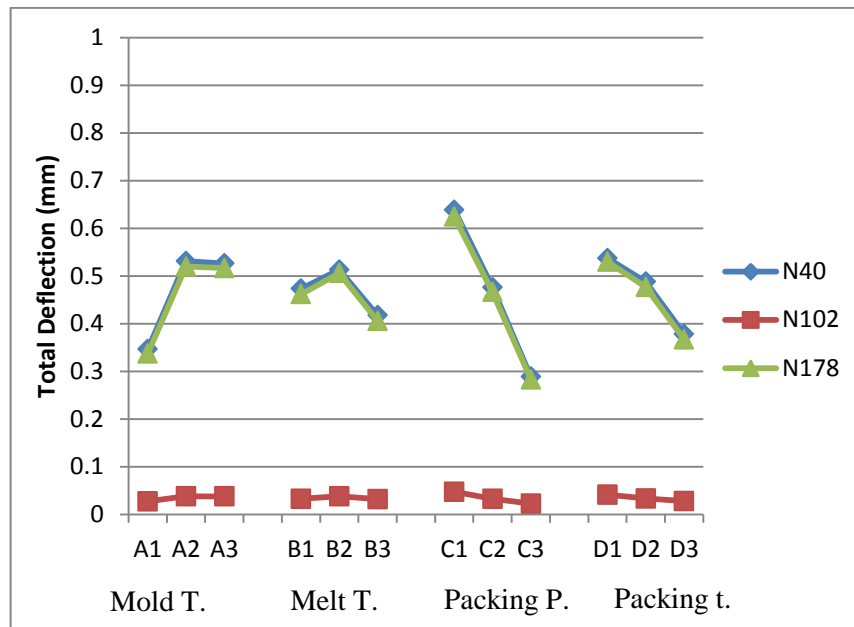


Figure 3-9 Total deflection result of PMMA dog bone (Numerical)

PC

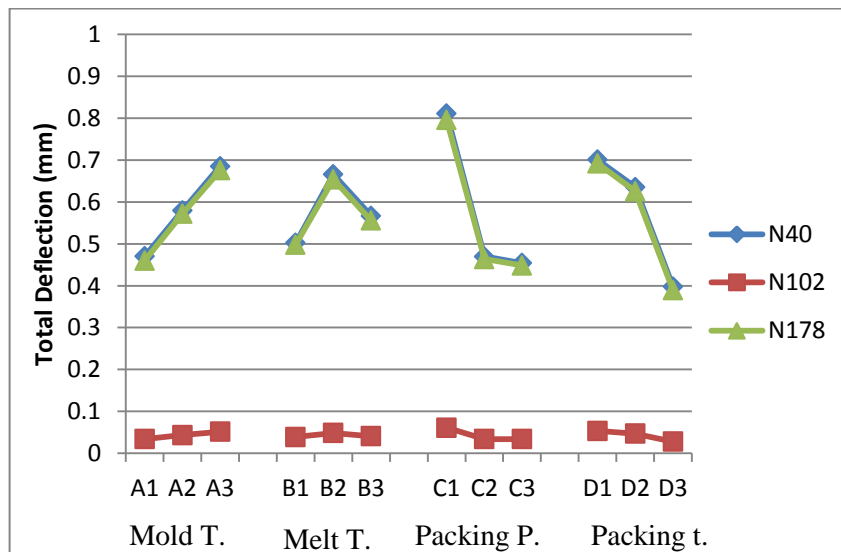


Figure 3-10 Total deflection result of PC dog bone (Numerical)

PS

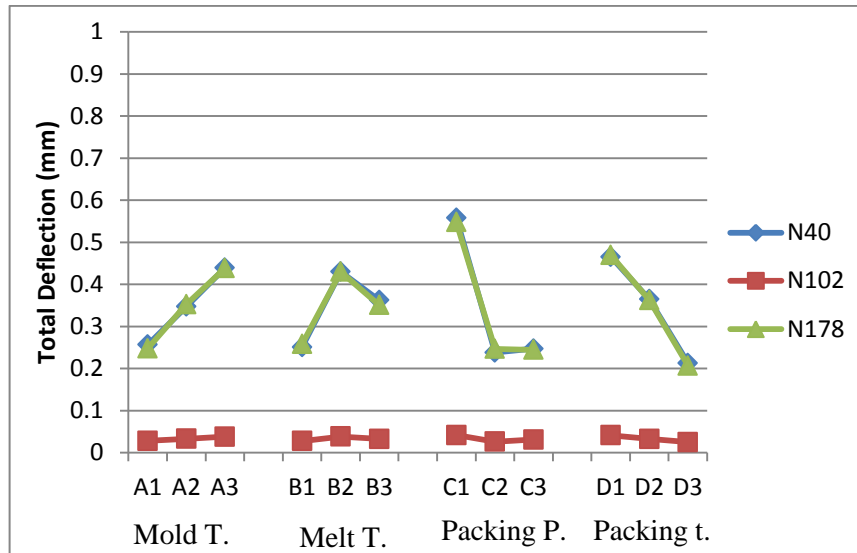


Figure 3-11 Total deflection result of PS dog bone (Numerical)

3.2.3 Part Mass

The total part mass is the final weight of the molded part from the process. Weight is one of the properties which represent product quality, especially in small electronic products [25]. The part mass results from numerical simulation are presented in Figures 3-12, 3-13, and 3-14 for the polymers considered.

PMMA

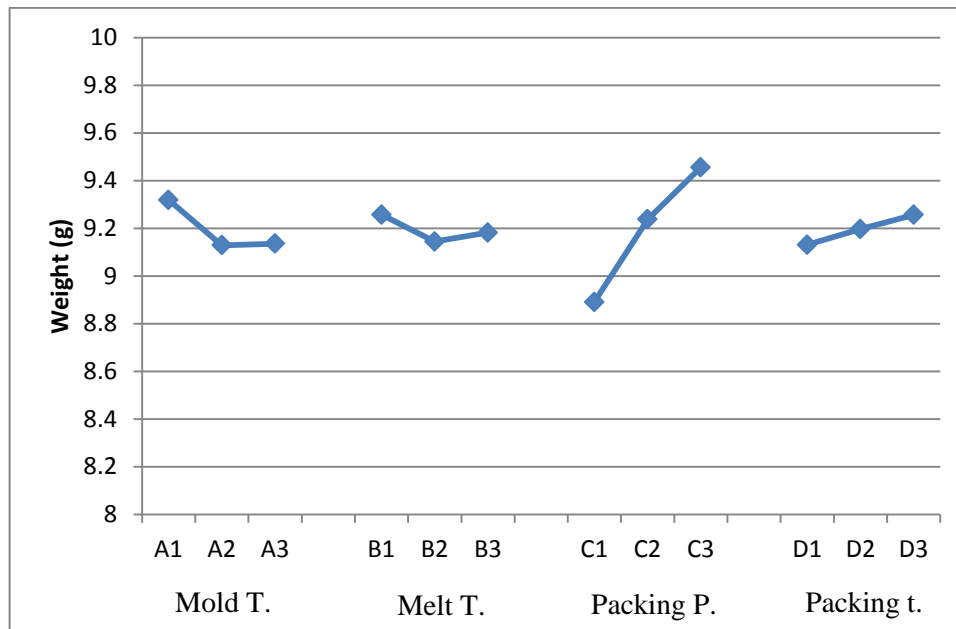


Figure 3-12 Weight result of PMMA dog bone (Numerical)

PC

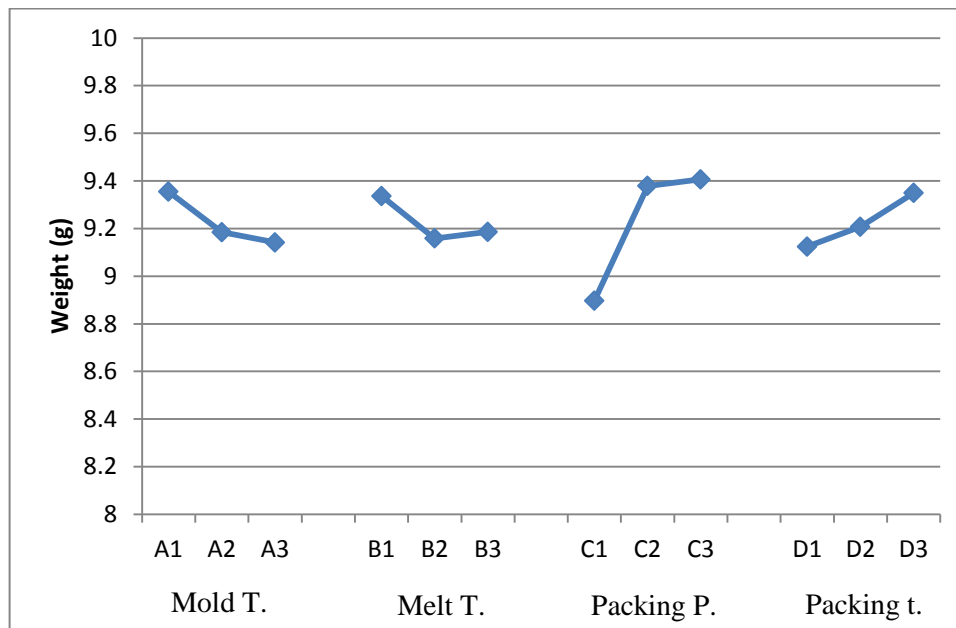


Figure 3-13 Weight result of PC dog bone (Numerical)

PS

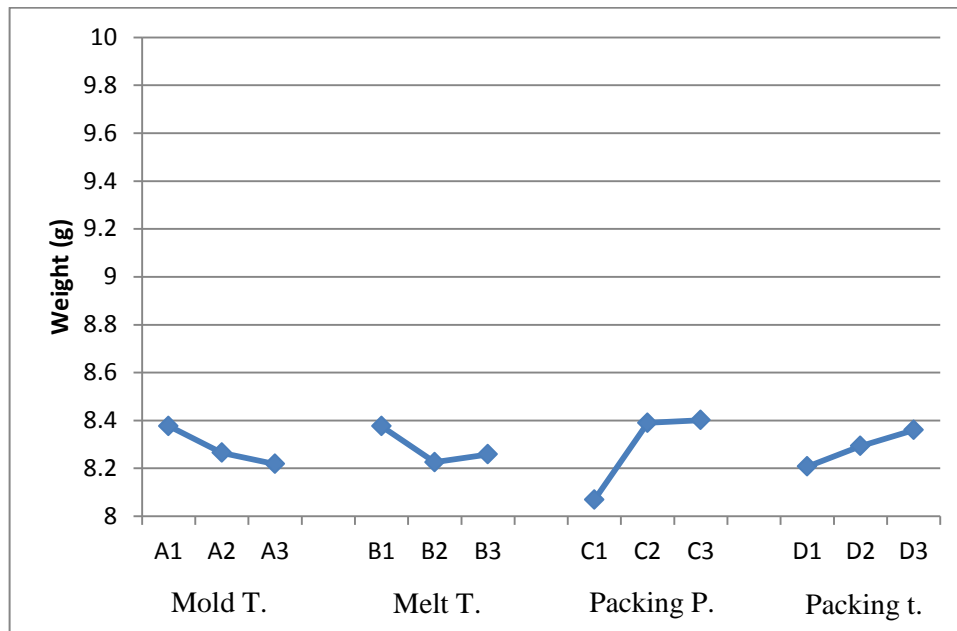


Figure 3-14 Weight result of PS dog bone (Numerical)

3.3 Experimental Investigation

The goal of this series of experiments was to investigate birefringence and strength of material result from processing parameters. Due to availability, the only resin used for the experiment was DOW general purpose polystyrene (GPPS) whose recommended processing conditions from INEOSNOVA are shown in Table 3-4 [26]. The mold and injection molding machine used to conduct the experiment were described in Section 3.1 (Figures 3.2 and 3.3). In the actual experiment, it was difficult to change the melt temperature frequently because it takes time to heat up or cool down the polymer melt in the machine. Furthermore, leaving the molten polymer in a barrel for a long time until the temperature changes can cause it to degrade. Therefore, melt temperature is not included as a parameter for the experiments. Taguchi method with $L9(3^4)$ orthogonal array was used again, but this time only three

parameters, including mold temperature, packing pressure, and packing time, are considered.

Table 3-5 shows all levels of each parameter selected for the experiment and the modified L9 array is shown in Table 3-6.

Processing Parameter	Unit	Value
Barrel Zone 1 Temperature (Feed)	F	340-390
Barrel Zone 2 Temperature	F	380-440
Barrel Zone 3 Temperature	F	425-490
Nozzle Temperature	F	400-450
Mold Temperature	F	50-160
Injection Pressure		Normally High
Back Pressure	psi	100-150
Screw Speed		Medium-High
Mold Shrinkage	in/in	.003-.007

Table 3-9 Recommended processing conditions for polystyrene [26]

Material	Parameter	Symbol	Level 1	Level 2	Level 3
PS	Mold Temperature (C)	A	30	50	70
	Packing Pressure (MPa)	B	38.40	56.32	76.80
	Injection + Packing Time (s)	C	5	10	15

Table 3-10 Parameters used for the experiment

Experiment	P1	P2	P3
1	1	1	1
2	1	2	2
3	1	3	3
4	2	1	2
5	2	2	3
6	2	3	1
7	3	1	3
8	3	2	1
9	3	3	2

Table 3-11 Modified L9 (3⁴) Orthogonal array

The ASTM D638 – Type I dog bone specimens were molded according to the information above. In order to get a steady part in each processing condition, the machine was running for ten cycles before the sample was taken into investigation. The Nissei machine was set up to have 40% of the maximum injection rate, approximately $20.4 \text{ cm}^3/\text{s}$, and V/P switchover at 95% volume filled which are consistent with the parameters of MOLDFLOW simulations in Section 3.2. The cooling time was reduced to twenty seconds which is more practical range and long enough for the molten polymer to completely solidify.

3.3.1 Birefringence

The technical information of polymer birefringence was presented in Chapter 2. Birefringence of PS dog bone specimens from nine experiments were investigated by using the polarizer shown in Figure 3-15. The specimens were viewed through a green 570 nm band-pass filter in order to see the fringes more clearly. The birefringence results from nine experiments are presented in Figure 3-16 respectively.



Figure 3-15 Polarizer used in the experiment

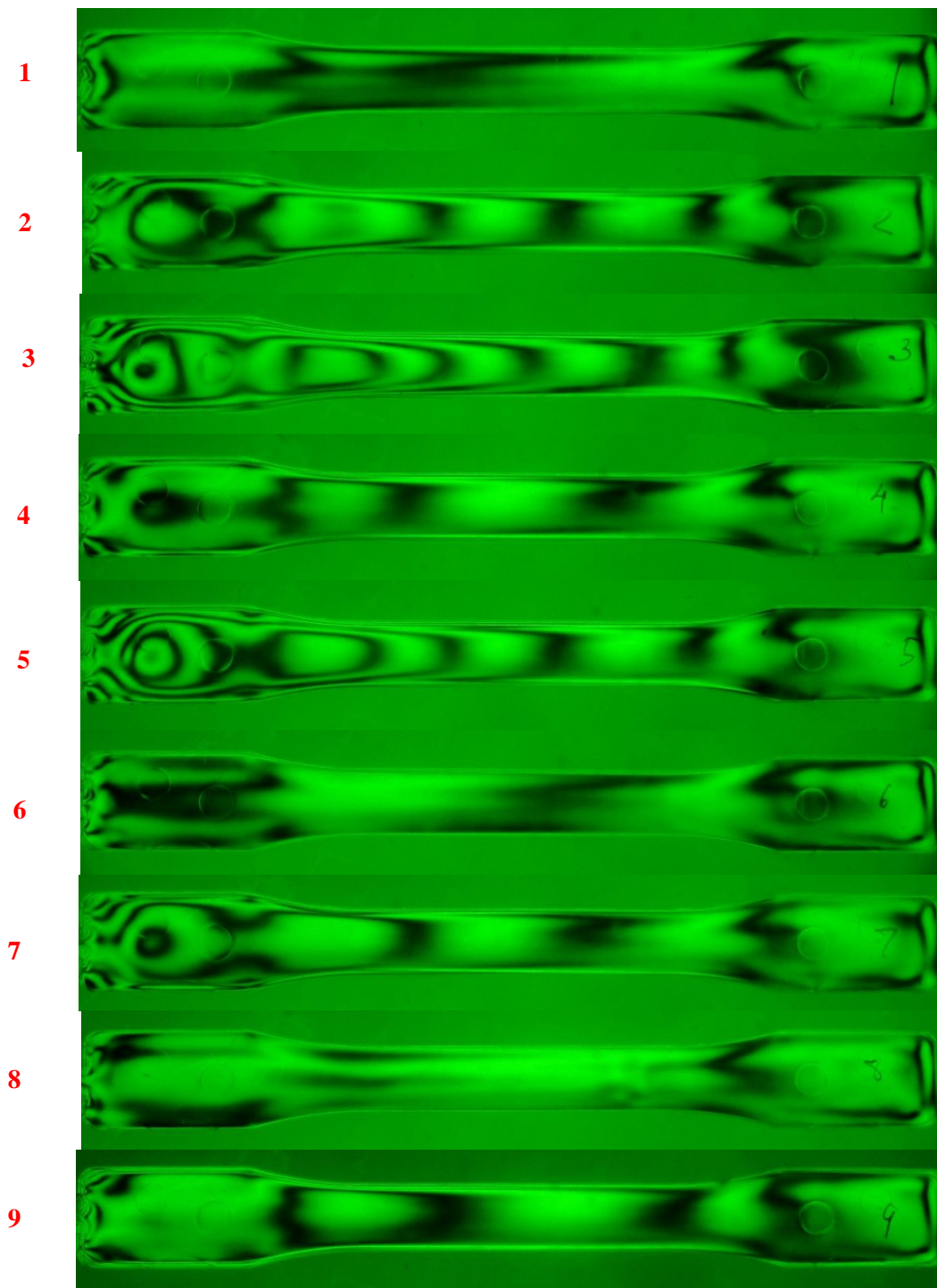


Figure 3-16 Birefringence result from Taguchi L9 method

After the samples were collected, the specimen from each experiment was used to calculate retardation from Equation 2-6. The retardation plots from nine experiments are presented in Figure 3-17. The horizontal axis represents the linear distance measured from the gate position.

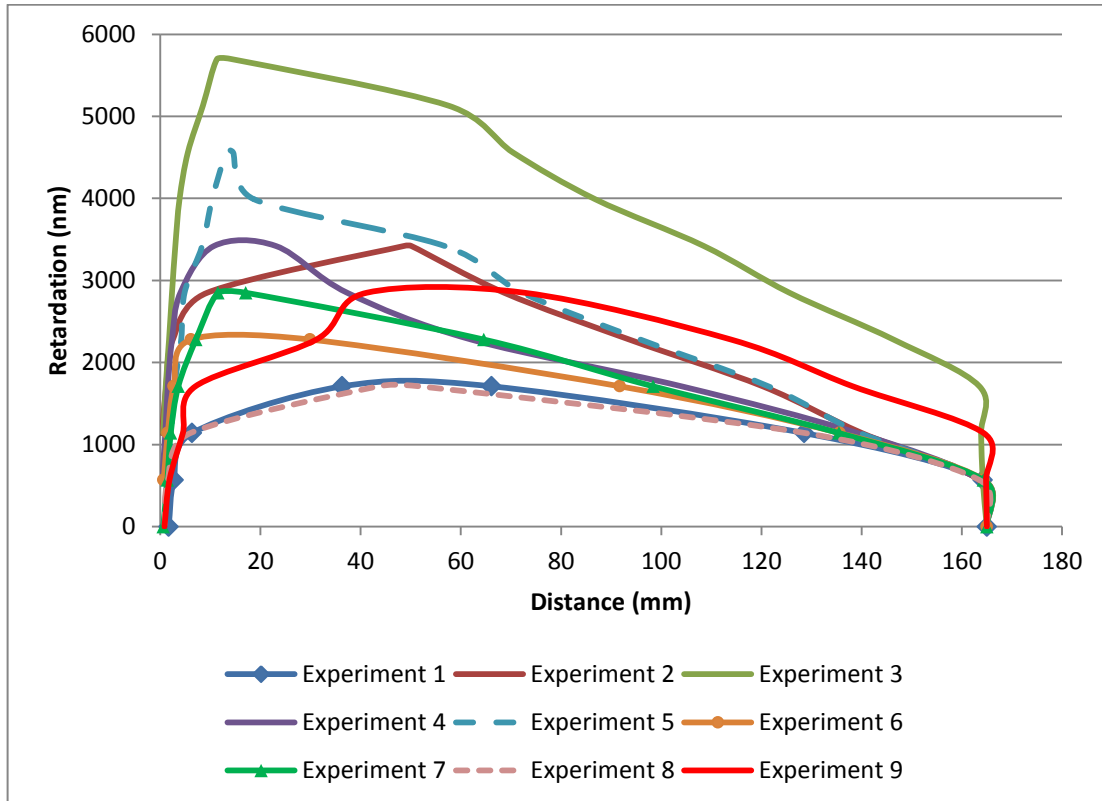


Figure 3-17 Retardation plot from the experiments

Retardation results from each experiment show significant difference in each experiment. To investigate the effect of the parameters on retardation, the maximum value of retardation from each experiment was collected to generate Taguchi plot as shown in Figure 3-18.

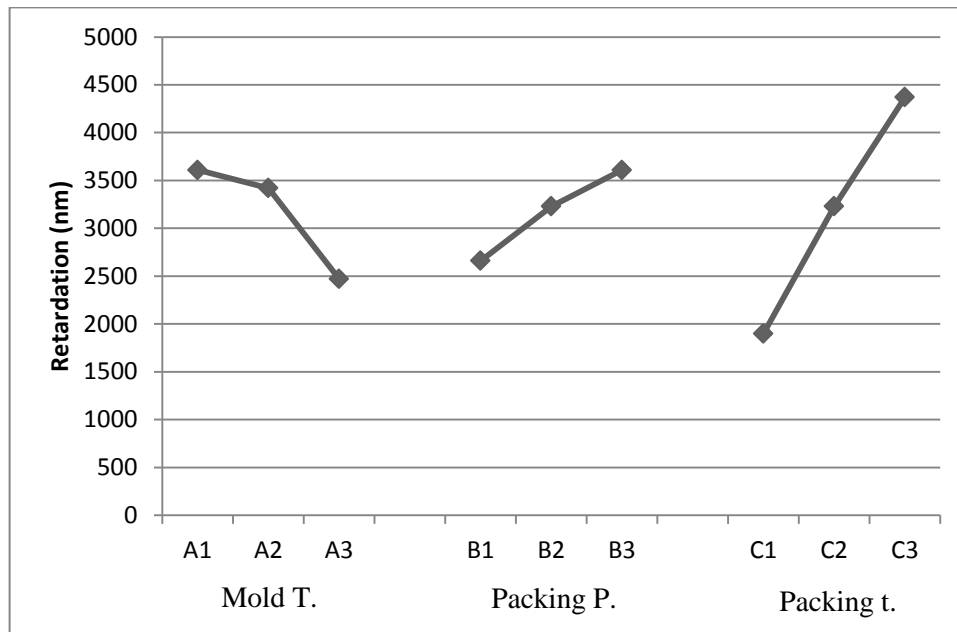


Figure 3-18 Maximum retardation result of PS dog bone (Experimental)

3.3.2 Tensile Testing

Five dog bone specimens from each experiment were brought to tensile test to investigate their strength properties from different processing conditions. Figure 3-19 shows the tensile test machine (MTI Phoenix, load cell capacity: 10,000 lbs) used for this experiment. The results from this experiment are average maximum tensile load and average maximum tensile stress as shown in Figures 3-20 and 3-21.

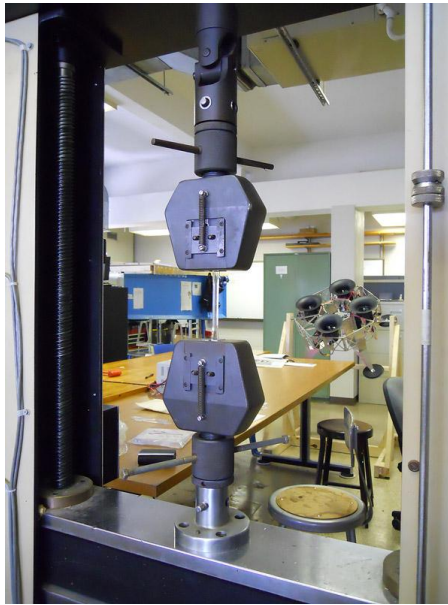


Figure 3-19 Tensile test equipment

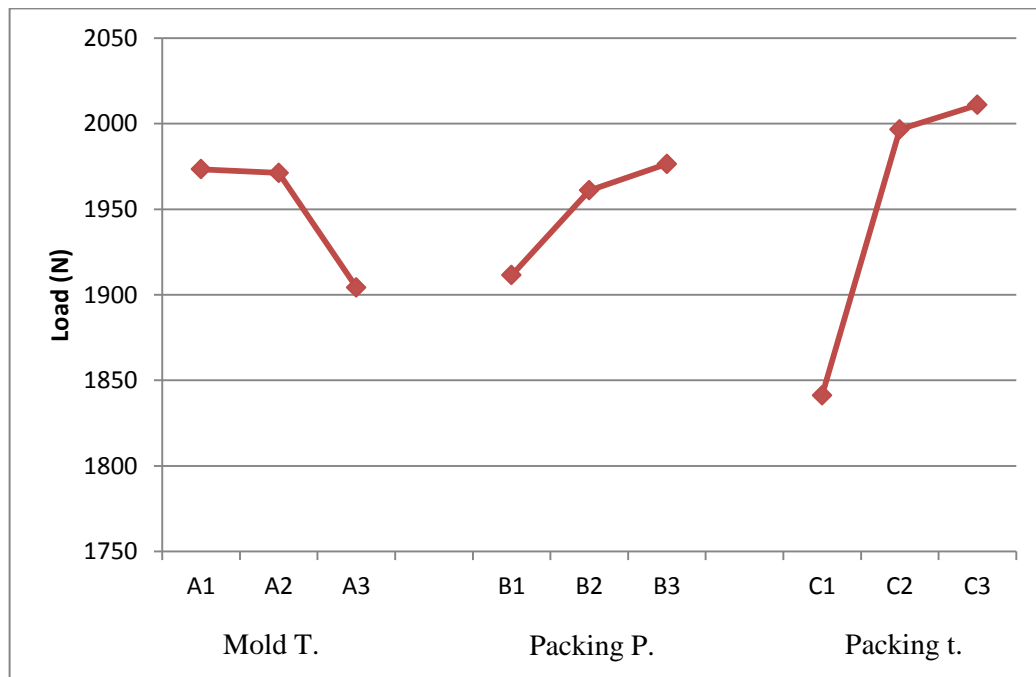


Figure 3-20 Average maximum tensile load result of PS dog bone (Experimental)

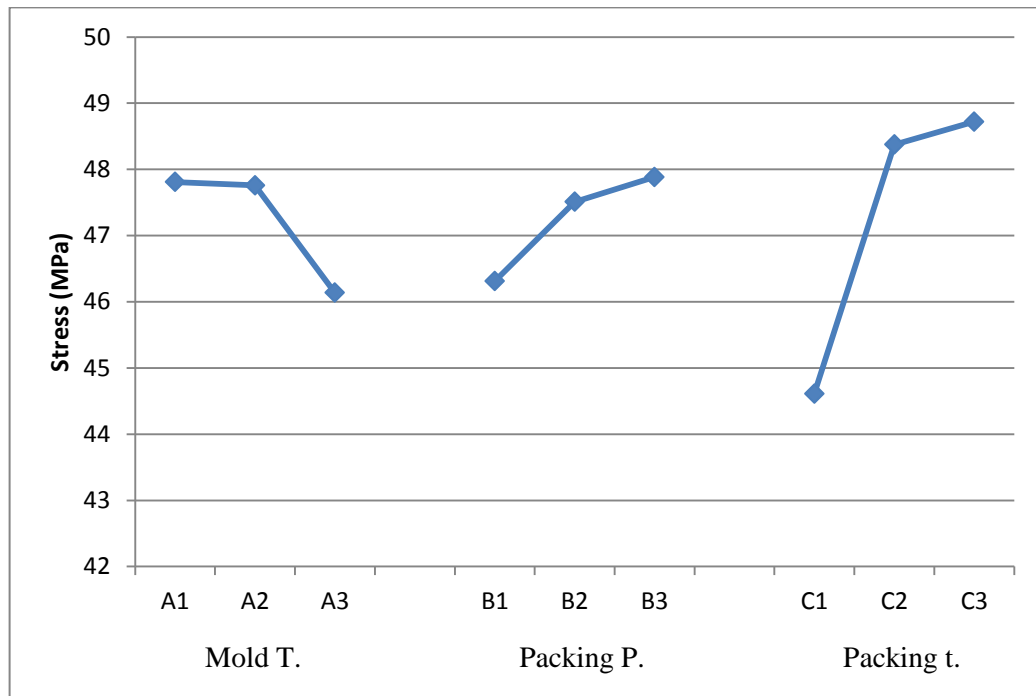


Figure 3-21 Average maximum tensile stress result of PS dog bone (Experimental)

3.4 Discussion & Conclusion

The results clearly show that selected processing parameters greatly influence the properties of molded products. Increasing packing parameters; i.e. packing pressure and packing time, tend to reduce the amount of shrinkage and deflection, but they also increase final weight. In contrast, increased packing parameters can cause higher molecular orientation in the part which results in higher birefringence and retardation. In addition, high molecular orientation makes the part to be stronger in the flow direction according to tensile test results.

Temperature parameters; i.e. melt and mold temperature, also have an effect on the part. Higher temperature will give the melt flow to have more relaxation time before it solidifies. The longer relaxation time means the material will have less residual stresses

which cause less birefringence and retardation too. However, higher temperatures tend to weaken the part and induce more shrinkage and deflection.

Since the two main factors which determine the quality of an optical polymeric part are final geometry and optical isotropy, the effect of parameters should be considered in relation to these two aspects. Obviously, for all materials, there is no parameter that can improve both measurements of optical quality. A better birefringence result generally comes with a worse final geometry, and vice-versa. Therefore, it is a challenge to compromise between these parameters for both quality aspects so that the machine will produce a final optical product with optimum quality.

This chapter provides the background information covering all important parameters to be considered when employing the melt modulation system to the injection molding machine. The next chapter explains about the design of melt modulation system used to investigate its capability to control the packing stage.

CHAPTER 4 – Design of a Compact Melt Modulation System for Packing Stage Control Applications

4.1 Introduction

A compact melt modulation system was designed to work with a cold runner mold. The A-series mold base size 9-7/8" × 8" from DME Company was selected to be assembled with the valve system. The A-series, shown in Figure 4-1, is a two-plated type which provides standard features for general purpose molding. From the figure, Both "A" and "B" plates are guided in the same alignment with pins and sockets. The "A" plate contains a sprue and connects to the injection nozzle when it is mounted to the injection molding machine. On the other hand, The "B" plate is coupled with the "A" plate on the opposite site. The ejection system used to remove the molded part is employed at the back of this plate. For this model, the "A" and "B" plates can be machined to have pockets to use with any type of core and cavity inserts.

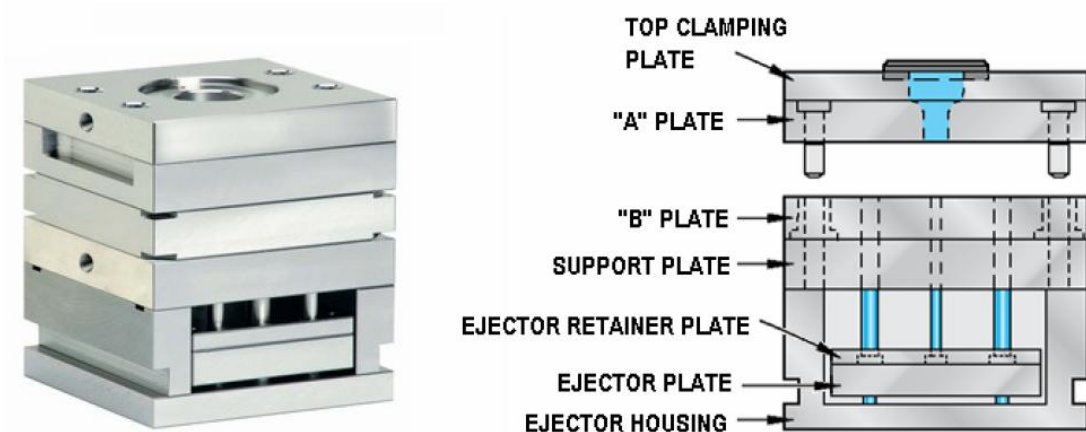


Figure 4-1 A-series mold base from DME Company [11]

The mold can mount to the Lehigh Nissei machine described in Chapter 3. In order to connect a compact melt modulation system to the mold, some parts of the mold were modified. The side view of complete mold base connected with a compact melt modulation system is presented in Figure 4-2.

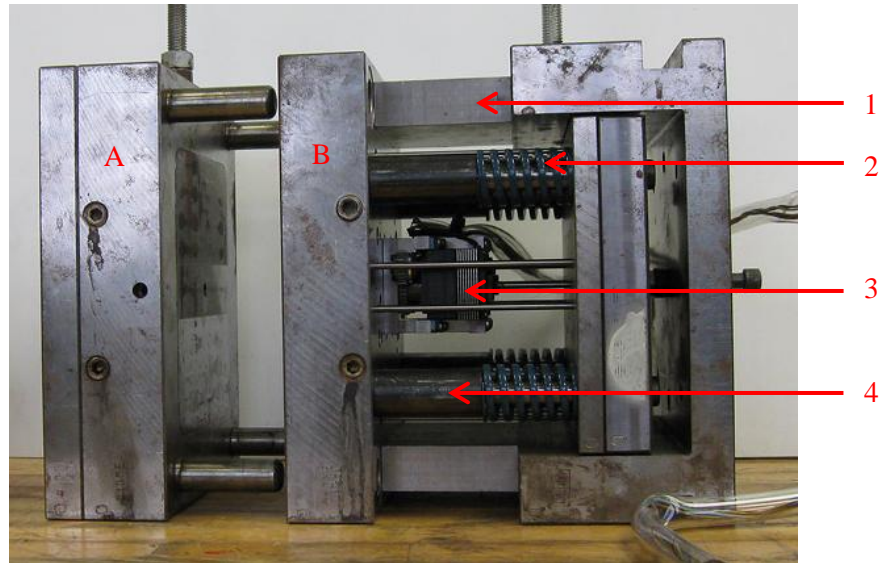


Figure 4-2 A-series mold base connected with a compact melt modulation system

The support plate was removed from the system and replaced by longer metal blocks (#1) to provide more space between the “B” plate and the ejector housing so that the compact melt modulation system actuator (#3) could be embedded at the back of the “B” plate. The sleeves (#4) were made to compensate for the longer distance and put along guided pins next to a die spring (#2). Therefore the ejector system works normally in this design.

Tantrapiwat used this compact melt modulation system to control melt flow during the filling stage. The mold inserts used in the experiments were spiral cavity and small dog bone (ASTM D638 Type-V) cavities [2] which do not suit the packing stage control

application due to the cold runner layout and the ejector system. With this in mind, a new mold insert was designed along with an enhanced actuator system to test the new application. The details of a new compact system design are presented in the next section.

4.2 New Melt Modulation System Details

The design development project was divided into three parts, the mold insert, the actuator system, and the valve port. The details of each part are given as follow.

4.2.1 Mold insert

To test optical properties of clear polymers, a lens-shaped part with a concave surface was designed to use with the application because lenses are the most common type of optical devices. The circular perimeter and concave surface represent the characteristic shape of a lens even though its dimension was not designed for any specific optical application. Figure 4-3 shows the drawing of the part design.

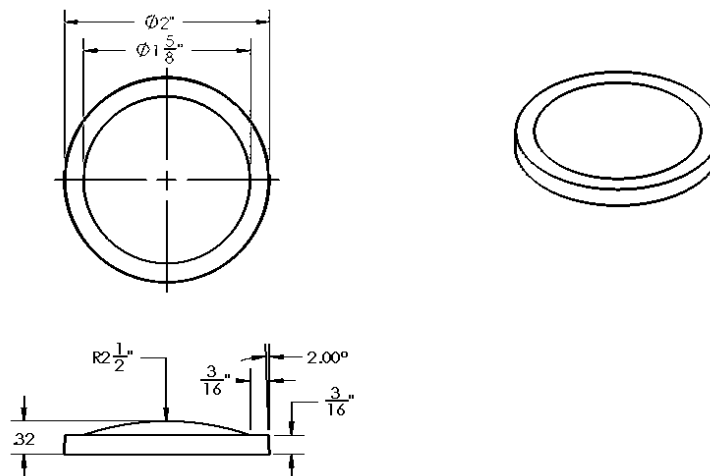


Figure 4-3 Drawing of lens-shaped part

Since investigating the capability to control packing parameters of the new compact melt modulation system was the main objective of this thesis, the pressure profile of the injection molding cycle needed to be measured to see the direct effect of the control valve on pressure in the cold runner system while it was turning. A pressure transducer from Kistler model 6159A was selected for this task. This model is suitable for monitoring both open and closed loop control process during the injection molding of thermoplastics [27]. Figure 4-4 presents the picture of the pressure transducer and its drawing. Technical data is presented in Table 4-1.

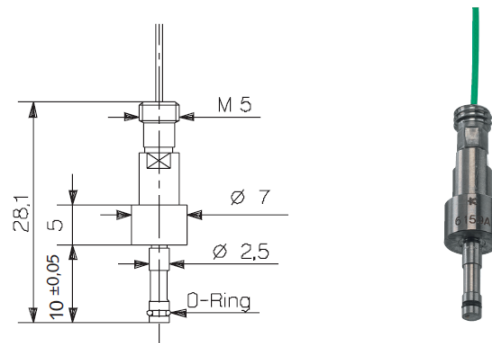


Figure 4-4 Kistler pressure transducer model 6159A [27]

Specification	Unit	Value
Range	bar	0-2,000
Overload	bar	2,500
Sensitivity	pC/bar	≈ -2.5
Linearity, all ranges	% FSO	$\leq \pm 1$
Operating Temperature Range		
Mold (sensor, cable, connector)	C	0-200
Melt (at front of sensor)	C	< 450

Table 4-12 Technical data of pressure transducer model 6159A [27]

The cold runner layout needed to be seriously considered for the new application due to a limitation of space of the pocket in the “B” plate, 6.5” × 5.5”. Since the Nissei machine can produce a two-level step function type packing profile, two valves were selected as being the most suitable for this situation. Even though the melt modulation system was previously developed to enhance filling stage, especially in family molding which cavities are not the same, in this case two identical lens-shaped cavities were chosen and symmetrically placed because their optical quality would be directly compared to each other to see the effect only from control valves.

To monitor the pressure profile of the cycle that results from the melt modulation system, pressure transducers were located to mount across the control valves so that they can measure the pressure drop. The length of the runners has to be long enough to let the melt modulation system and transducers mount into it. However, it should be as short as possible to reduce pressure drop of melt flow along the way before it reaches the cavities. Because the pressure transducer has a flat front, the 5° trapezoidal runner with standard 1/8” diameter was selected as the best choice for this mold. The end of the transducer is able to be mounted at the same level with the bottom of the runner as illustrated in Figure 4-5.



Figure 4-5 Pressure transducer position with the trapezoidal runner

Technical drawing of a mechanical part, likely a bracket or plate, showing dimensions and tolerances. The part is rectangular with rounded corners and features two circular holes, one on the left and one on the right. A horizontal slot is located between the two holes.

Dimensions and Tolerances:

- Overall width: $6\frac{1}{2}"$
- Distance from left edge to center of left hole: $3\frac{1}{4}"$
- Overall height: $5\frac{1}{2}"$
- Distance from top edge to center of left hole: $2\frac{3}{4}"$
- Distance from center of left hole to center of right hole: $1"$
- Distance from center of right hole to right edge: $1\frac{1}{8}"$
- Distance from bottom edge to center of right hole: $1\frac{1}{4}"$
- Radius of top corners: $R\frac{1}{8}"$
- Radius of bottom corners: $R\frac{1}{2}"$
- Radius of circular holes: $\phi\frac{1}{8}"$
- Slot width: $.02"$

67

4.2.2 Actuator System

The original compact melt modulation actuator designed by Tantrapiwat used a spur gear transmission between the output shaft of the HITEC actuator and the valve stem because the valve stem needs an ejector pin in the middle as described in Section 2.4.2. Since the development of valve return cycle and new control methods in Section 2.4.4, the weak spot of solidified runner disappears, so there is no need to use an ejector pin in the valve center anymore. The valve stem can be directly connected to the output shaft from the actuator. From this idea, the original compact system in Figure 4-7a can be reduced to be even smaller system as in Figure 4-7b whose the size of the entire unit is approximately 35% less than the original design [2].

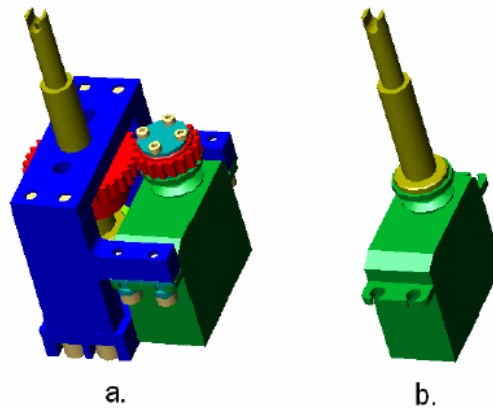


Figure 4-7 Original compact system and the direct coupling valve design [2]

The direct coupling valve design in Figure 4-7b needs a coupler between the spline-ended output shaft from the actuator and the valve stem. A coupler from ServoCity-Robotzone, LLC. was selected for this task [28]. It is machined from 6061 T6 aluminum which has high reliability. The coupler can handle 1,500 oz-in of torque without slipping

which satisfies the melt modulation application. Figure 4-8 shows the drawing of the chosen coupler, and Figure 4-9 presents the assembly of the new direct coupling valve design for the compact melt modulation system.

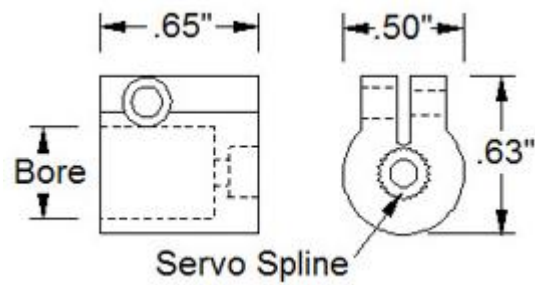


Figure 4-8 Drawing of a valve coupler [24]

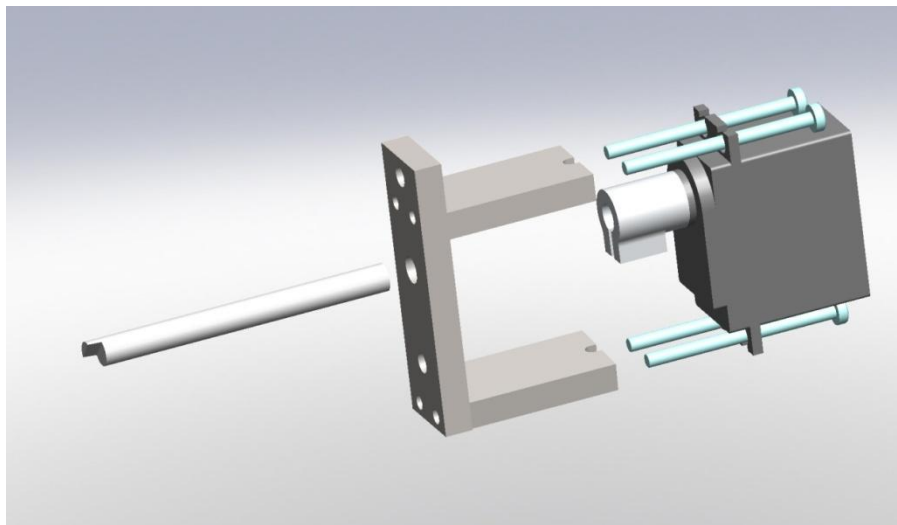


Figure 4-9 Direct coupling valve design

In addition to changing the driving mechanism in Figure 4-7, the melt modulation system was re-configured. Originally, the compact melt modulation system was embedded at the back of the “B” plate as in Figure 4-2. The valve stem has only one task which is to

restrict the cross-sectional area of the runner. In certain processes, the “B” plate is heated up to relatively high temperature. Heat from the “B” plate will conduct to the actuator system and could cause some damage to the electronic device. Tantrapiwat solved this problem by inserting an insulation sheet between the HITEC actuator and the case [2].

The new configuration was inspired by the enhanced multiple valve design developed by Tantrapiwat [2]. The compact melt modulation system was re-located to the back of the ejector plate. To provide the space at the back of the ejector plate, the sleeves (#4 in Figure 4-2) were moved out of the system, and the die springs (#2 in Figure 4-2) were changed to be shorter. Therefore, when the cycle ends and the machine pushes the ejector plate forward to kick the solidified part out, the valve stems will act as an ejector pin itself to help eject the solidified runner. The diagram of the new configuration design is presented in Figure 4-10 as follow.

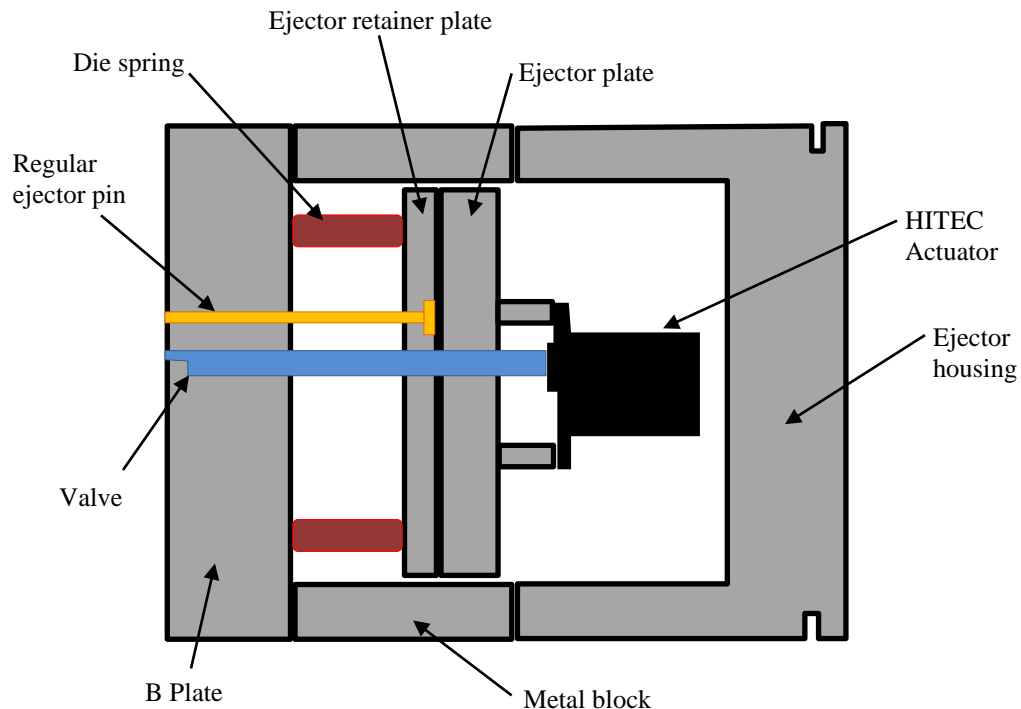


Figure 4-10 New configuration of the compact system

4.2.3 Valve Port

The details regarding original valve port design are presented in Section 2.4 in Chapter 2. All of them exhibited an undesired quick opening behavior for the filling stage which means they have a short range of effective operating range of valve angle as shown in Figure 4-11 [2].

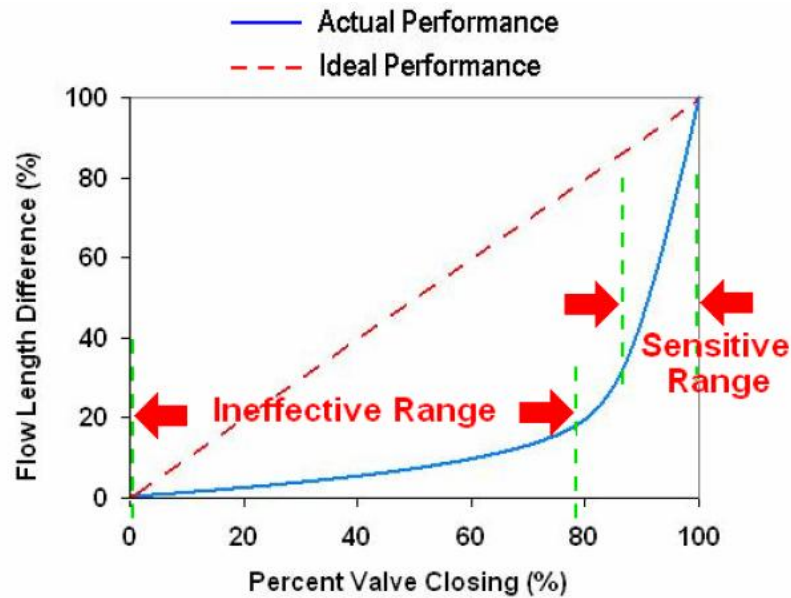


Figure 4-11 Ideal performance and effective range of original valve ports [2]

An improved valve port can be created by adapting an eccentric plug valve instead of rotary plug type. The eccentric valve port has similar geometry to the original design, but it has only one plug. To work with the cold runner, the eccentric valve has to be placed offset from the middle. The configuration of the new eccentric valve is presented in Figure 4-12.

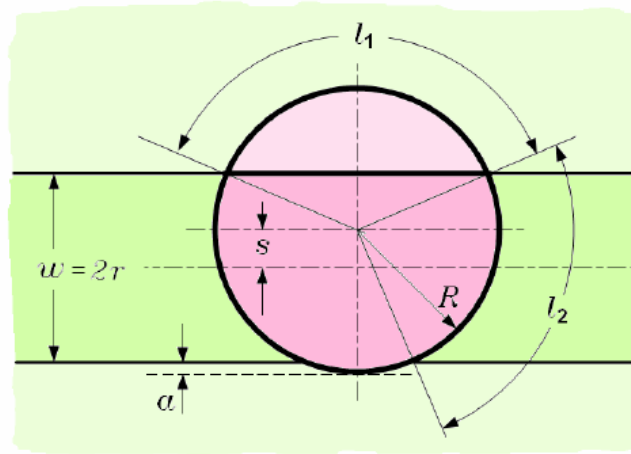


Figure 4-12 Eccentric valve port configuration

According to the new configuration, the operating angle of the eccentric valve port can be determined as:

$$\theta = \sin^{-1}\left(\frac{r-s}{R}\right) + \sin^{-1}\left(\frac{r+s}{R}\right) \quad (4-1)$$

where r is the half of the cold runner width, R is the valve port radius, and s is the offset distance from the center of the runner. In order to operate the valve from the fully open position until fully closed position, the design parameters have to be selected to make the curvature l_1 longer than l_2 as in Equation 4-2.

$$l_1 = 2R \cos^{-1}\left(\frac{r-s}{R}\right) \geq l_2 = R\theta \quad (4-2)$$

To effectively use the eccentric valve port with the filling stage, the range of operating angle should be optimized to be maximum as possible in order to make the flow characteristic more controllable. According to Equation 4-1, reducing the valve radius, R , and

the offset distance, s , could provide the better operating angle result. Tantrapiwat performed a numerical simulation to test the flow behavior of the eccentric valve port compared to the original design, the result shows that flow characteristic of the new eccentric port has more linear response which is better [2].

The eccentric valve port was selected to use to investigate the packing stage control capability of the melt modulation system in this thesis due to its better performance and simplicity to manufacture. It can be machined to have the same profile as the runner from the THX-typed ejector pin from DME company [29] by common operation. The major concern to apply the valve to the experiment is the valve must close the runner perfectly. With the 1/8" trapezoid runner previously described, the two design parameters, i.e. valve radius and offset distance have to be chosen to satisfy that requirement. Theoretically, the zero valve seating distance, α , could shut the flow off, however, there is a chance that the plug could not perfectly seal the runner due to dimensioning tolerance. To ensure the runner is fully closed, the value of α should be greater than zero as following:

$$\alpha = R - r - s > 0 \quad (4-3)$$

The 0.25" valve radius was selected as same as the original valve stems, while the offset distance was selected to be 0.02". Table 4.2 presents all parameters of the eccentric valve port used for the packing stage control application.

Parameter	Unit	Value
Valve Diameter, R	in	0.25
Half of Runner Width, r	in	0.0684
Offset Distance, s	in	0.02
Range of Operating Angle, θ	degree	67.79
Curvature $l1$	in	0.293
Curvature $l2$	in	0.149
Valve Seating Distance, α	in	0.037

Table 4-13 Parameters of eccentric valve port

4.3 Conclusion

All of the important components are shown in this chapter. The information contains the idea of design and technical specification. The lens shaped part was designed in order to test the optical results, and two eccentric valves were employed in the mold to work with the trapezoidal shaped cold runner system. All components could then be assembled together and used to test the capability to control the packing stage during injection molding processes.

CHAPTER 5 – Design of Experiment and Numerical Simulation of Valve-runner System with Lens-shaped cavity

5.1 Introduction

After the entire new Melt Modulation system was design and fabricated as discussed in Chapter 4, Chapter 5 presents the design of experiment for the equipment in order to propose the testing guideline for packing stage control application. In addition, a series of numerical simulations is included in this chapter. The objective of numerical simulations is to investigate the effect of the Melt Modulation system on the cold-runner system designed in Chapter 4. The machined lens-shaped cavity and runner are shown in Figure 5-1. Pressure drop across the valve and the molded part quality are the main investigated properties that result from processing parameters, including valve angle, packing pressure, and packing time. As was done in Chapter 3, MOLDFLOW was used as a simulation tool for all of the studies.

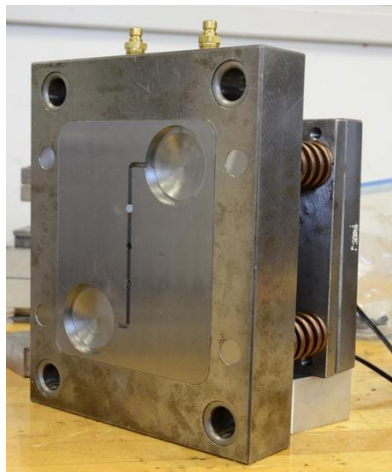


Figure 5-1 Cold runner system for packing stage control application

5.2 Design of Experiment

The set of experiments would be conducted using the same Nissei injection molding machine shown in Chapter 3 with the specifications presented in Table 3-1. Since the main purpose of the experiment is to control the packing stage of optical product (lens) molding cycles, transparent materials used for optical product manufacturing were selected. These included Plexiglas® V920 (PMMA) [30], Styron CALIBRE™ 300EP-22 (PC) [31], and Styron® 685D (PS) [32]. Recommended processing conditions are presented in Table 5-1 as follow:

Parameter		Material		
		PMMA	PC	PS
Barrel Temperature	Rear (C)	204	252-300	200-215
	Middle (C)	210	269-313	215-230
	Front (C)	216	278-322	230-245
	Nozzle (C)	210	276-319	230-245
Mold Temperature (C)		65-85	70-120	15-65
Injection Rate (% of Maximum)		50	50	50
Cycle time (s)		120	120	120

Table 5-14 Recommended processing parameters of PMMA, PC, and PS [30, 31, 32]

The mold and melt temperatures are suggested to be relatively high in order to have the polymer melt solidify slower so that the valve would have a longer operating time range during the packing stage. In addition, high mold temperature improves optical property because it produces higher surface gloss, reduces molecular orientation and helps minimize

flow marks and weld lines. Generally fast injection rate is recommended because it provides better uniformity. However, fast injection rate can be applied for only certain cases depending on gate size and location, so 50% of maximum injection is a safe starting parameter. Then it can be increased later to the fastest rate that produces acceptable part quality [32]. Cycle time heavily depends on part thickness. The more thickness the part has, the more cycle time it requires to provide better geometric tolerance [30].

The packing profile of the Nissei machine can be set as a two-level step function such as that shown in Figure 5-2. Each level can be set from 0%-100% of maximum packing pressure that the machine can produce.

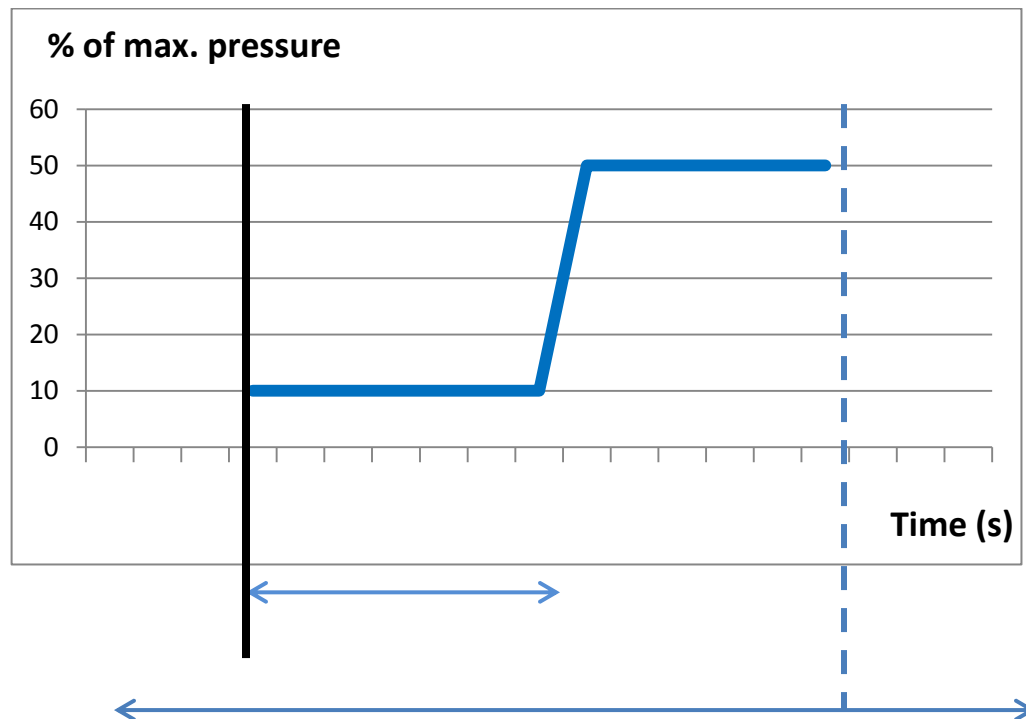


Figure 5-15 Packing profile of Nissei machine

Before conducting the experiment, the packing range should be defined. The first step is trying to fill both cavities to 95% of the total volume with 100% opened runner and no packing pressure. Next is to increase the packing pressure equally for level 1 and 2 until both cavities are completely filled. Packing pressure can be increased until the cold-runner system starts to flash. Therefore the packing pressure range would start from the level that completely fills both cavities and end before reaching the level that causes flashing.

In order to control two cavities to have different packing profiles, after filling 95% of total volume with fully open runners, the valves need to be rotated differently from each other during the packing stage before the polymer solidifies. The control valve can completely shut the runner off or rotate to certain angle to restrict the pressure. The set of experiments can be divided into three sections to see the effect from three control methods, including packing pressure control, packing time control, and valve angle control.

The first method, packing pressure control, was used with the packing profile which has two levels of packing pressure. The concept is to shut one valve off at a specific time during the first level of packing pressure. So the remaining pressure during packing stage will apply to only the other cavity. Figure 5-3 shows the example set of experiments to test packing pressure control approach with various initial packing pressures. The red dash line represents the time when the control valve shuts the runner off.

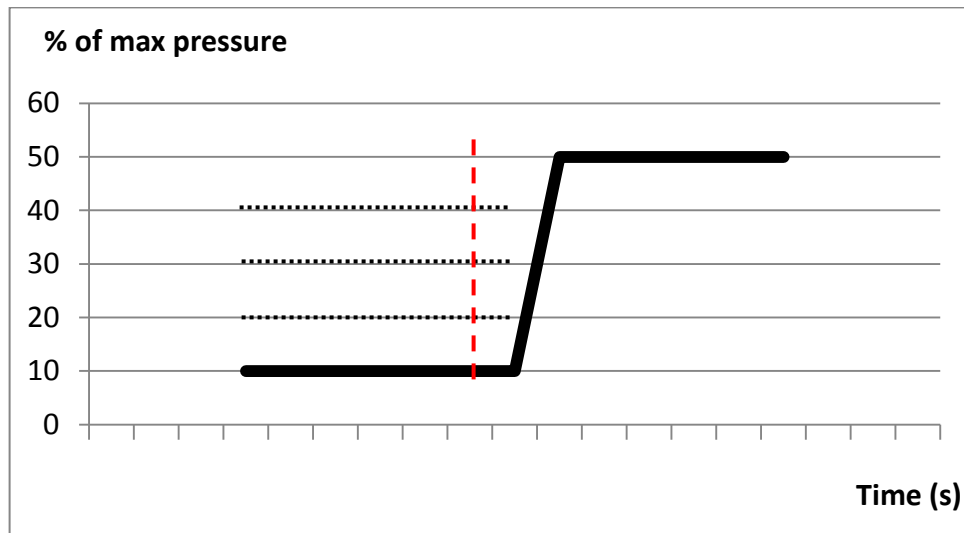


Figure 5-3 Testing approach for packing pressure control

The packing time control method applies to constant packing profiles during the packing stage. One valve is controlled to shut the runner off at a specified packing time so that two cavities will be different. The concept of this idea is shown in Figure 5-4.

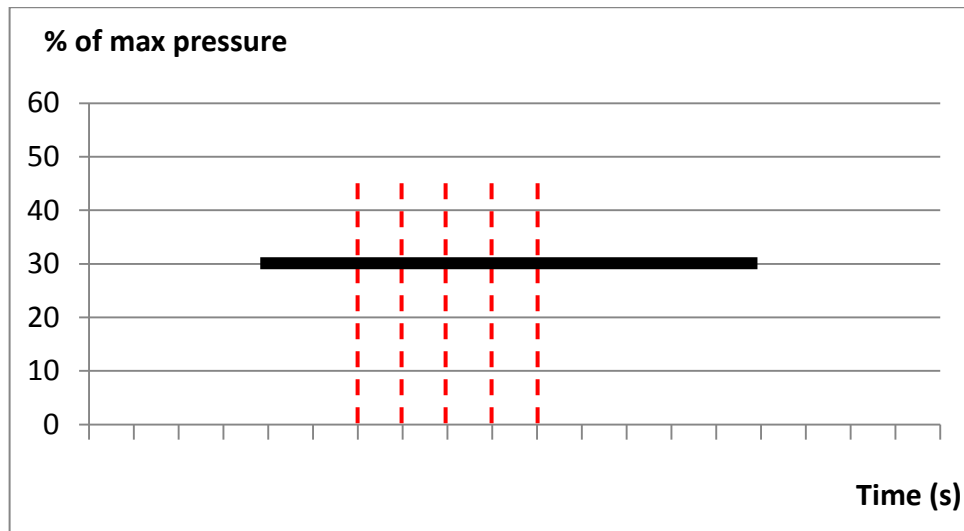


Figure 5-4 Testing approach for packing time control

The valve angle control method also applies to constant packing profiles. Instead of shutting the runner off completely, at a specific packing time the valve turns to a specific angle to reduce the cross-sectional area of the runner. The smaller area should result in less amount of packing pressure passing through the valve.

All three control methods described above are just the initial testing approach to make sure that the Melt Modulation system can control the packing stage of injection molding processes. If all three methods work well, they can combine together to create many new control techniques which will generate various pressure profiles in each cavity. The pressure measured by pressure transducers and the birefringence in the molded part will be considered as a result from packing stage control.

5.3 Numerical Simulation Setup

The 3D models of the cold runner system, shown in Figure 4-6, were created and imported into Moldflow. There are four models which have different valve angles. Since the range of operating angle, θ , is 67.79° , the four models are determined by dividing the range of operating angle into four steps, 16.984° each. From the fully open position, the runner is considered to be 100%. By rotating the valve with the angle step three times, other models are 75%, 50%, and 25% respectively. Figure 5-5 illustrates the control valve position of the four models which have different valve angle. Because Moldflow cannot analyze a transient process, i.e. turning the control valve during the cycle, all control valves need to be set at specific angle before a cycle starts. Then if two valves have different angle before injection, both cavities will be unequally filled. This imbalanced filling opposes the packing stage control concept because both cavities should be completely filled first before rotating the

valves during the packing phase. Because of this reason, all models were created to have only one side in order to avoid unbalanced filling.

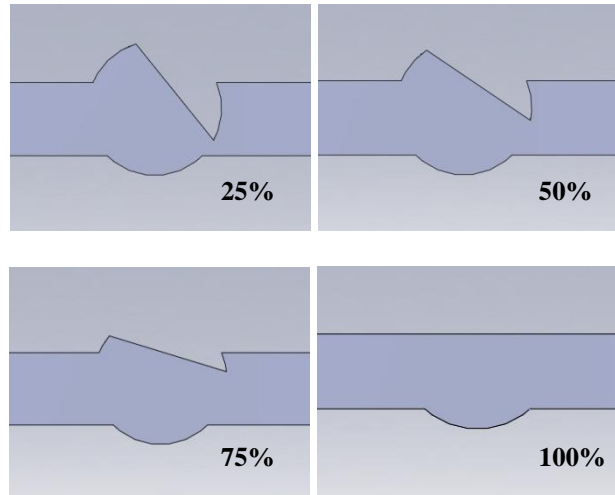


Figure 5-5 The runner at control valve position of each model

All models were meshed with a 3D approach [24] to provide the most delicate result. A 0.7 mm global edge length was applied through the models except the valve position in 25% and 50% model that use 0.3 and 0.1 mm global edge length due to smaller cross-sectional area. Figure 5-6 presents the example 3D meshed model of the 25% model used in this chapter. Three common optical polymers were chosen for the numerical simulation; Plexiglas[®] V920 (PMMA), Styron CALIBRE[™] 300EP-22 (PC), and Styron[®] 685D (PS). Processing parameters were set according to Table 5-1. Packing pressures were 30%, 45%, and 60% of the maximum pressure the Nissei machine can produce [23] with a packing time of 15 seconds, 40 tons of clamping force, and V/P switchover at 95% volume filled. The pressure results were obtained using the red dot positions shown in Figure 5-7, P1 and P2, the same as the actual pressure transducer positions.



Figure 5-6 25% model with 3D meshing

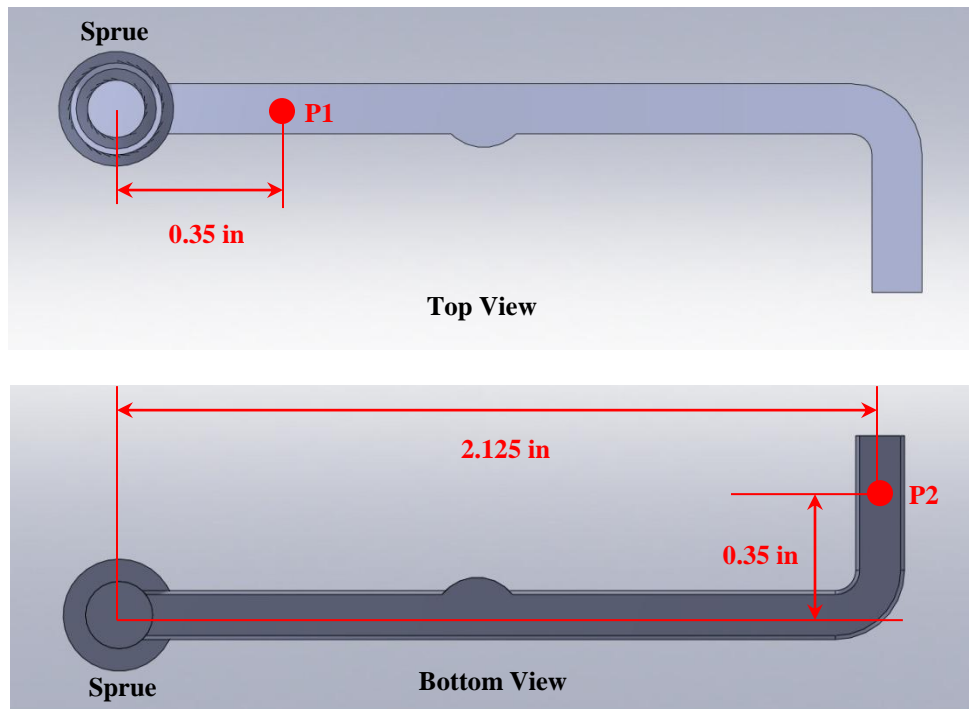


Figure 5-7 Pressure transducer positions

5.4 Numerical Simulation Result

5.4.1 Different valve angle

The difference of pressure, ΔP , between two positions shown in Figure 5-7 can be calculated by P1-P2. The data from the four models in Figure 5-5 is plotted as a function of time from the cycle starts until the end of the packing stage. The plots show the effect of initial valve angle on pressure drop of each polymer during the cycle. From the simulation result, the filling stage lasts about 0.4 second and the packing pressure is 30% of the maximum the Nissei machine can produce. The difference of pressure results for PMMA, PC, and PS are shown in the Figures 5-8, 5-9, and 5-10 respectively.

PMMA

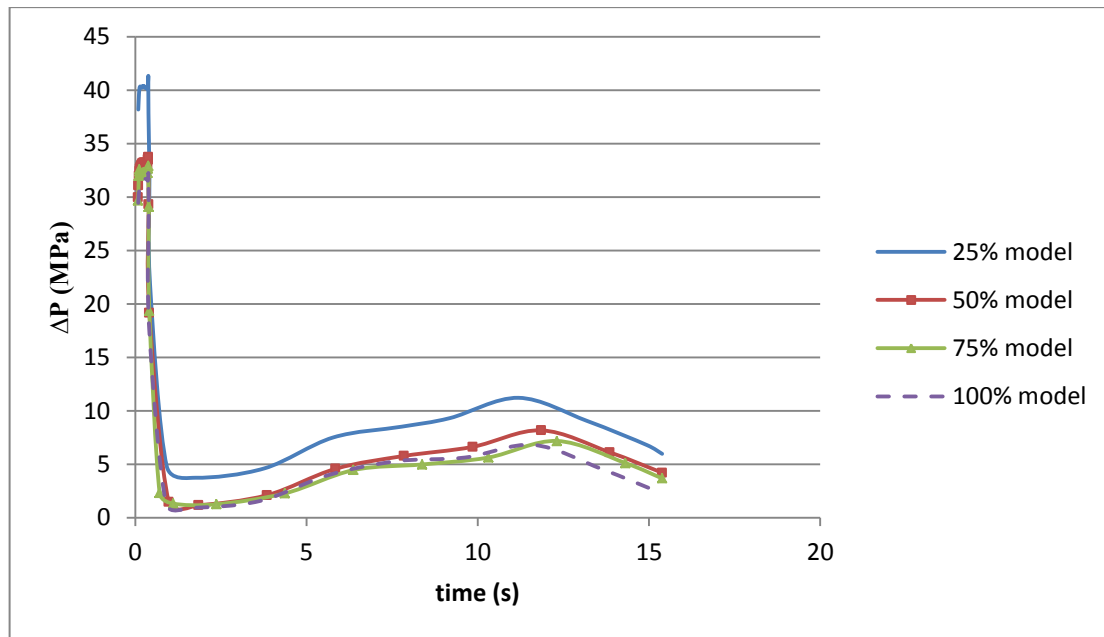


Figure 5-8 Pressure difference result of PMMA with four valve angles

PC

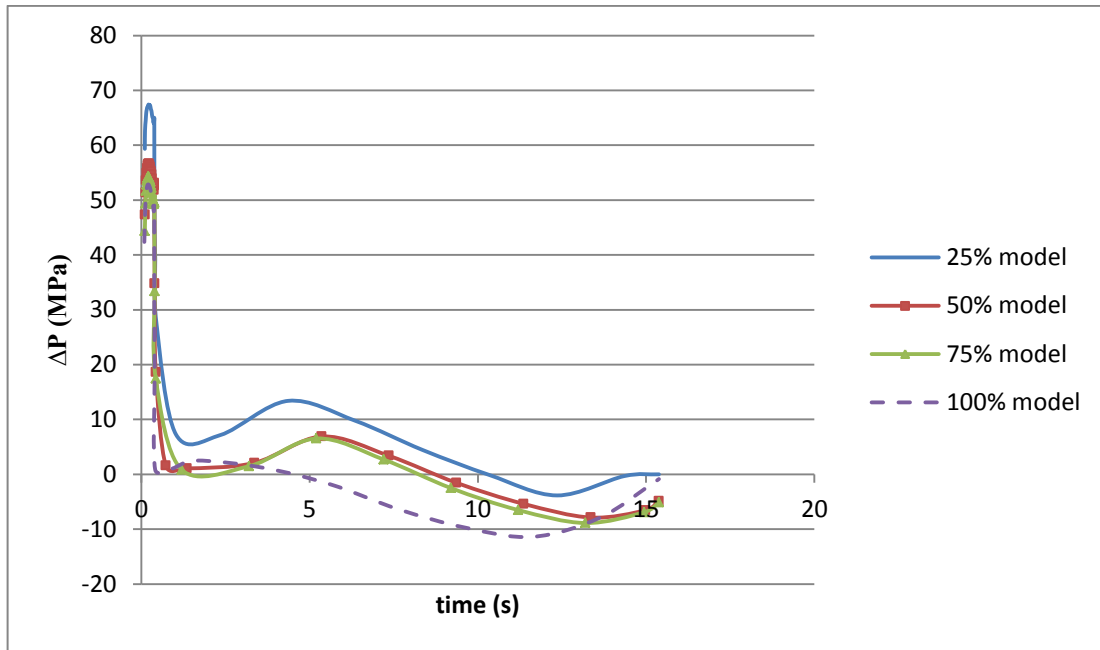


Figure 5-9 Pressure difference result of PC with four valve angles

PS

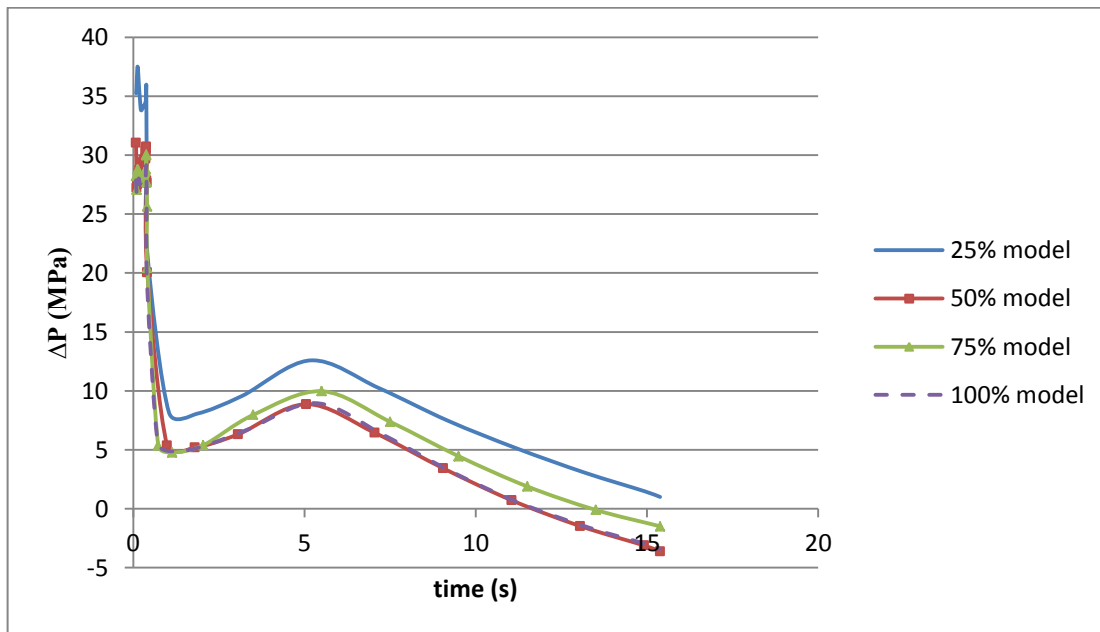


Figure 5-10 Pressure difference result of PS with four valve angles

5.4.2 Different packing pressure

The difference of pressure between P1 and P2 from the 25% model is plotted as a function of time. The plots show the effect of various packing pressure on pressure drop of each polymer during the filling & packing stage. The selected values of packing pressure are 30%, 45%, and 60% of the maximum. The difference of pressure results for PMMA, PC, and PS are presented in the Figures 5-11, 5-12, and 5-13 respectively.

PMMA

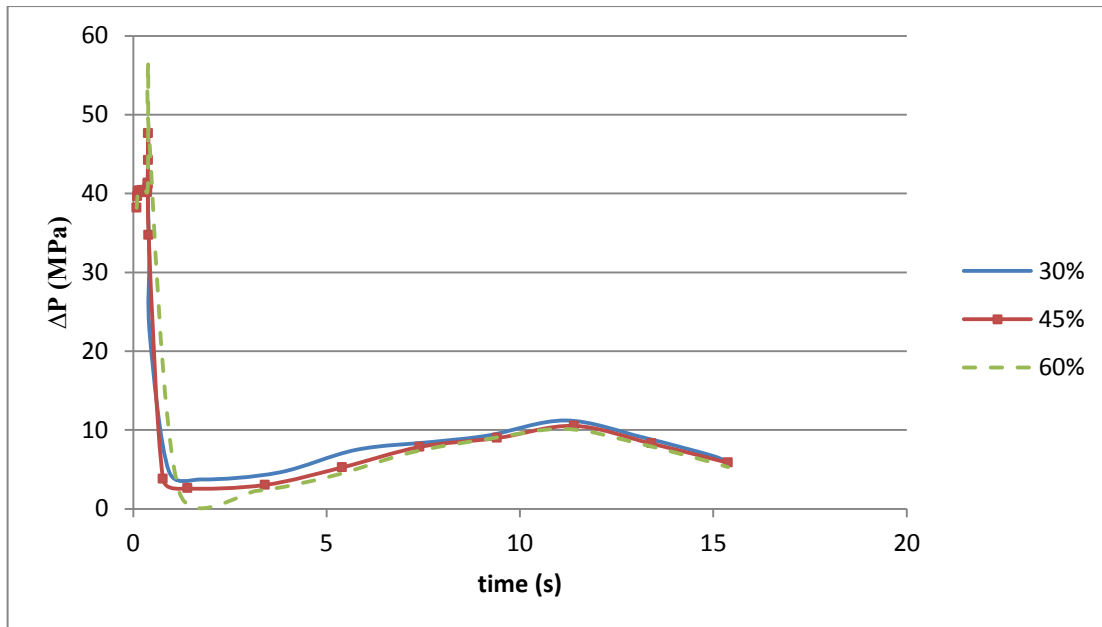


Figure 5-11 Pressure difference result of PMMA with three levels of packing pressure

PC

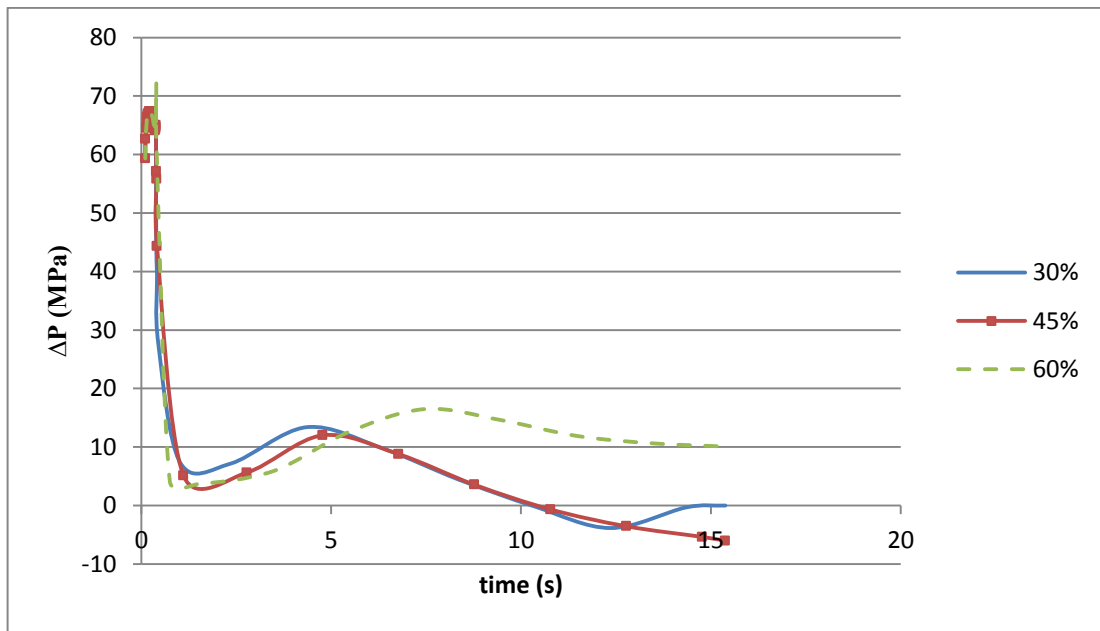


Figure 5-12 Pressure difference result of PC with three levels of packing pressure

PS

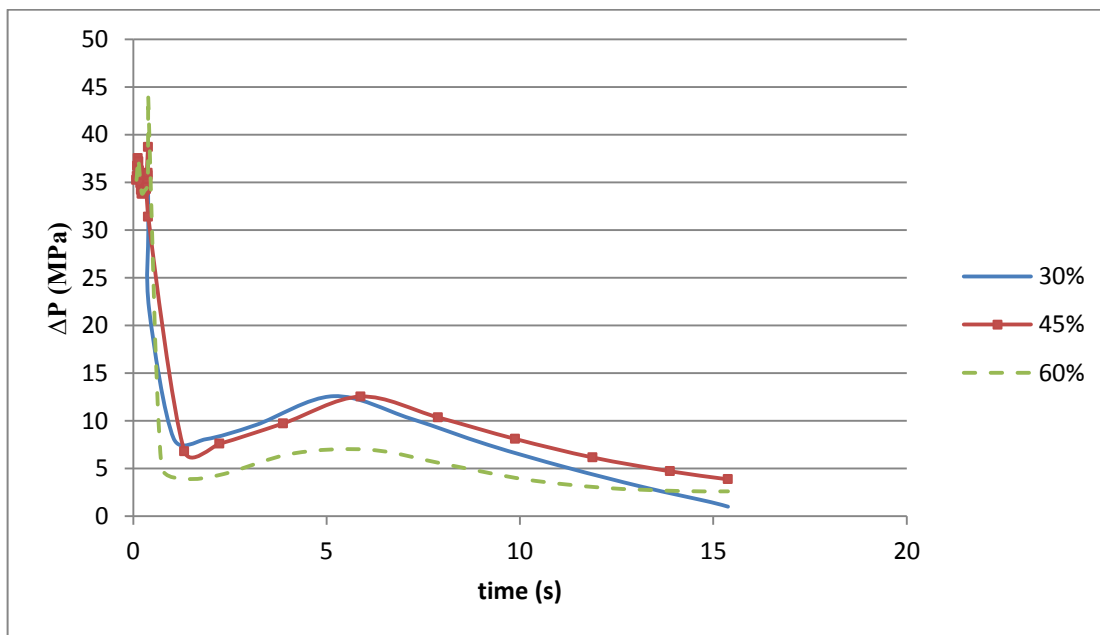


Figure 5-13 Pressure difference result of PS with three levels of packing pressure

5.4.3 Pressure at the cavity entrance

The following plots show the pressure result at the P2 position of the four models for the entire cycle. The pressure at the injection location (sprue) was also added to be a reference. The pressure at the cavity entrance for PMMA, PC, and PS is presented in Figures 5-14, 5-15, and 5-16 respectively.

PMMA

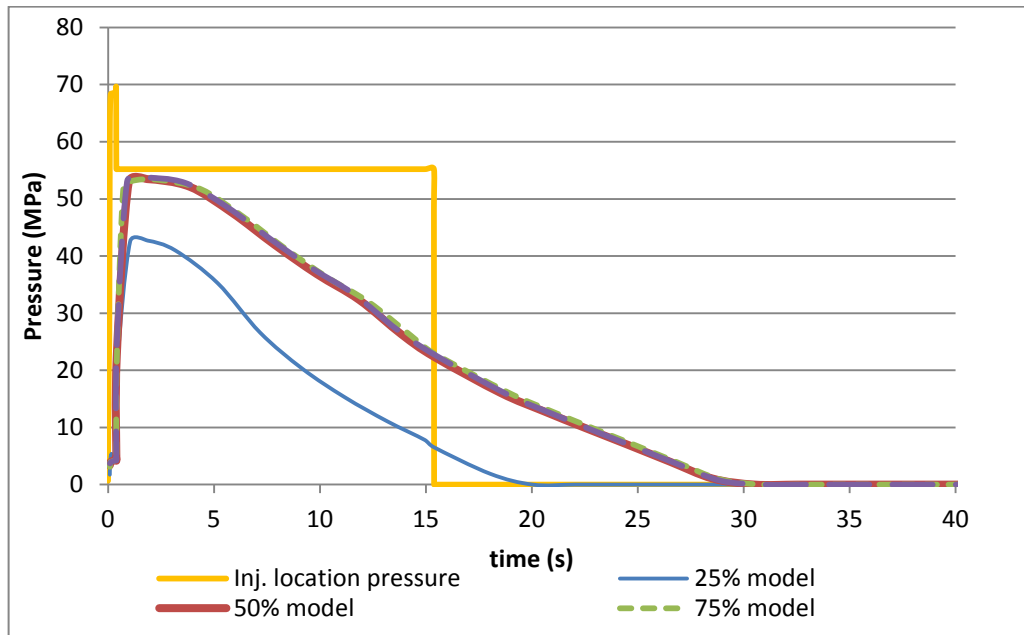


Figure 5-14 Pressure at the cavity entrance (PMMA)

PC

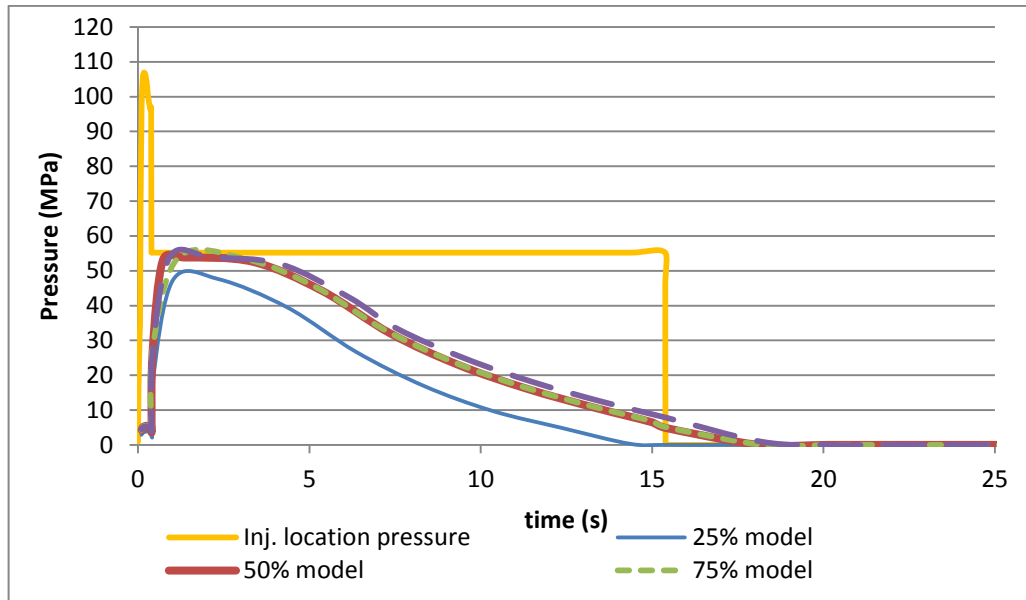


Figure 5-15 Pressure at the cavity entrance (PC)

PS

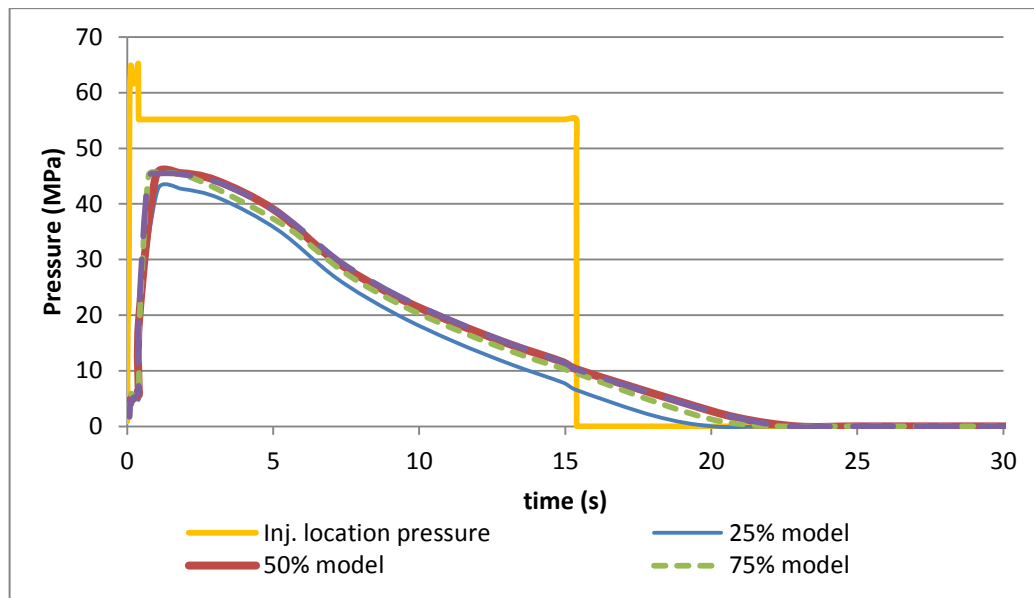


Figure 5-16 Pressure at the cavity entrance (PS)

5.4.4 Average volumetric shrinkage

The following plot shows the average volumetric shrinkage percentage at the end of the molding cycle as a function of different valve angle. The investigated shrinkage is at the center of the concave surface of the molded lens because it is the thickest location in the part.

Figure 5-17 presents the results for all polymers; PMMA, PC, and PS.

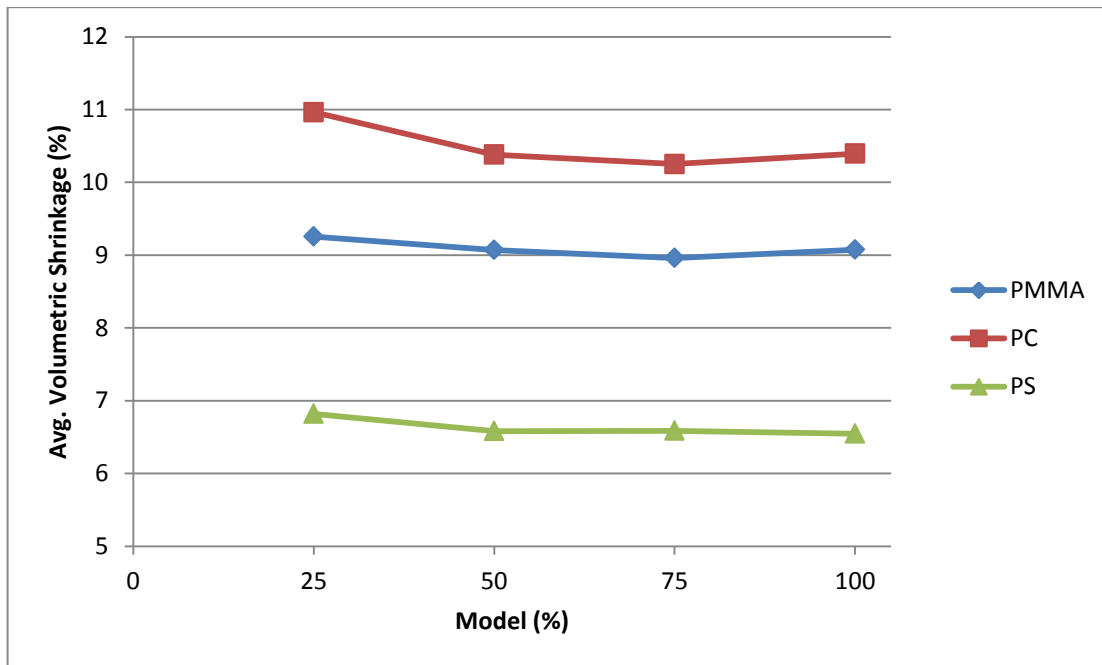


Figure 5-17 Average volumetric shrinkage result at the center of the molded lens

5.5 Discussion & Conclusion

The results in section 5.4 show that the initial valve angle influences the pressure profile of the molding cycle. From part 5.4.1, the smaller cross-sectional area of the runner increases the pressure drop across the valve. Pressure drop is obvious when the control valve rotates into the position as in the 25% model. On the other hand, 50%, 75%, 100% model did not provide the significant difference of pressure drop. So the control valve might possess the quick-opening behavior for the packing stage control application too, i.e. the pressure drop rapidly increases when the valve is nearly closed. If this happens, the control valve will have only a small effective operating range.

From section 5.4.2, the plots conclude that more packing pressure will slightly reduce pressure drop across the valve. With more pressure drop occurs when the runner is nearly closed, the molded lens has slightly more average volumetric shrinkage at the center. However, since packing pressure is applied when the melt stops flowing, the valve angle therefore has a small effect on the pressure profile due to static pressure distribution [2]. So the result from both section 5.4.1 and 5.4.2 do not provide much pressure drop for all conditions.

From the reasons above, if the control valve has a quick-opening characteristic for packing stage control and produces only insignificant pressure difference when turned to specific angle, this approach will not be a recommended technique to control the packing stage. The small operating range causes difficulties to control the valve because valve position has to be very precise. By adapting the Bang-Bang technique [2] to this application, turning the valve to fully closed position may be a more effective way to control packing pressure.

CHAPTER 6 – SUMMARY AND CONCLUSION

6.1 Research Summary

Since first invented in 90's, the Melt modulation technique has been developed in many aspects. From the first costly and bulky design, it has been improved to be smaller, more efficient, and cheaper. The first applications used with the technique are to control melt flow by a fixed-angle method in order to properly fill a family mold, and to control a weld line position. Tantrapiwat enhanced overall system and developed new control methods for filling stage (Bang-Bang and Hybrid) which greatly promote Melt modulation technique to an industry level.

In this thesis, Melt modulation technology has been expanded in terms of its capability to now independently control both the filling & packing stages of an injection molding cycle. According to the research objectives presented in Chapter 1, all of them have been accomplished. The project progressed from Tantrapiwat's previous research in Chapter 3 in order to **investigate the effect of processing parameters on the optical quality of an injection molded product**. The series of numerical simulations and experiments were conducted. The results show that packing parameters, including packing pressure and packing time, seriously affect the optical quality of molded parts in terms of final geometry and optical isotropy. However, changing processing parameters cannot improve both aspects of optical quality in one condition. When Melt modulation system is tested in the experiment, if the result insists that the system can generate different packing profile to a different cavity, it implies that

optical quality can be controlled by the control valve. By using this concept, family molding for optical products can be improved.

In Chapter 4, the previous compact system developed by Tantrapiwat was examined. The compact system was modified and improved to be smaller and simpler for assembly as in Figure 6-1.

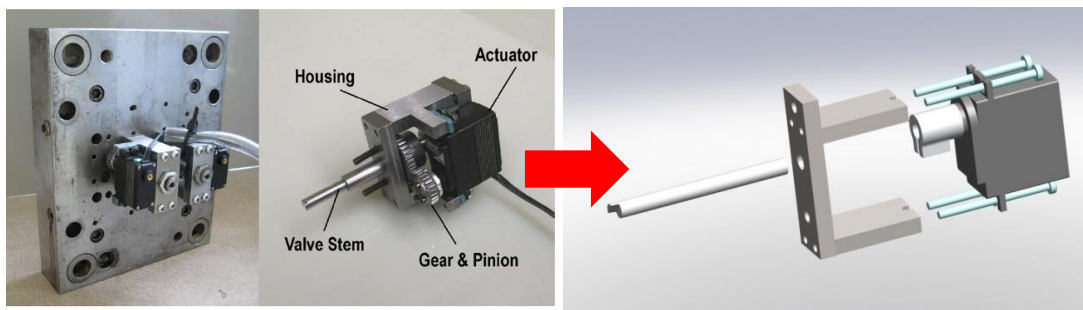


Figure 6-1 The first compact system and the developed prototype

In addition, the new compact system also has more functionality. Because an eccentric valve stem does not have an ejector pin at the center like the original rotary plug valve, it is important to make the system eject solidified polymer at the valve port as the previous model does. By moving the embedded position from the back of the B plate to the back of the ejector plate, the new compact system can perform as an ejector pin as well to help the mold eject a solidified part. The new configuration is shown in Figure 6-2.

A completely new cold runner system which has lens-shaped cavities was fabricated to use with packing stage control application. The mold insert was presented in Figure 5-1. Pressure transducers which are the extra equipment for this application were attached at three positions in order to measure the pressure during the cycle. All of works in Chapter 4 have

fulfilled the second objective which is to **modify the previously developed melt modulation systems and mold for packing stage control purposes.**

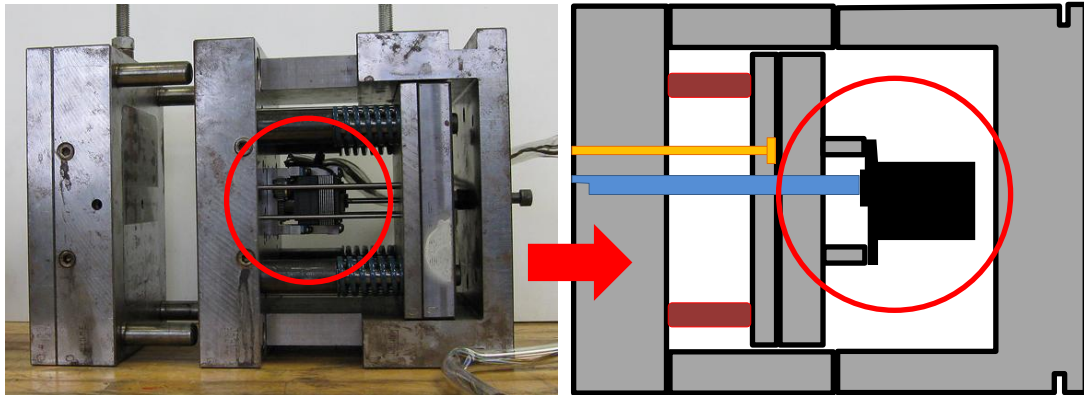


Figure 6-2 Developed configuration of the compact system

Chapter 5 proposes the experimental guideline for packing stage control applications according to the system fabricated in Chapter 4. Packing pressure and packing time are the main variables to control. Four 3D models with different valve angles were created in the next part to **investigate the capability of melt modulation system to control a pressure profile in a packing stage by numerical simulation.** Pressure drop across the valve was the main parameter used to judge the capability to control packing pressure. The valves were set at specific angles for the entire cycle. Even though the result shows that there is a pressure drop after the valve position, there is not a huge difference of pressure drop when rotating the valve to different angles. The valve position that makes the runner have the smallest cross-sectional area (25% model) produces the most obvious pressure drop, while the others (50%, 75% and 100% model) produce almost the same result. From this characteristic, the control valve seems to have a quick-opening behavior in the packing stage control application too. The result also shows that controlling packing stage is material sensitive. All optical

polymers used in the simulation (PMMA, PC, PS) have different pressure profiles although they are processed by the same processing conditions. Since Moldflow cannot simulate a transient process by shutting the valve off during packing analysis, the Bang-Bang method needs to be tested in the experiment only.

6.2 Proposed Future Work

According to Chapter 5, a Melt modulation experiment can continue in the packing stage control application to investigate its further capability by using the mold in Figure 5-1. Instead of using ineffective traditional fixed-angle method as the numerical simulation in Chapter 5, the Bang-Bang method should be applied. By switching a valve position to fully closed, most of the pressure should be blocked across the valve. Then a huge pressure drop will occur. The experiment guideline for the Bang-Bang method is presented in Section 5.2. In addition, a detailed valve characteristic in packing stage needs to be experimentally determined. The experiment begins with setting valve angle to be fully open. Then set the injection molding machine to fill both cavities to 95% of total volume. During packing stage, rotate one control valve to a specific angle at certain packing time to cause a pressure drop. In order to get a precise valve behavior, the operating range should be divided into at least ten intervals (10% each). The result from this experiment will determine whether the control valve possesses a quick-opening characteristic for both filling & packing stage control applications.

A control valve position is another variable to be investigated. From the numerical simulation in Chapter 5, the result shows that pressure drops faster at the area just after the valve port compared to pressure in the cavity, especially in the 25% model. So pressure in the

cavity may drop faster if the control valve is very close. The new 3D models can be created by using the same lens-shaped cavity with a straight runner. The valve position is varied from the gate position connected to the cavity to the farther position along the runner as shown in Figure 6-3.

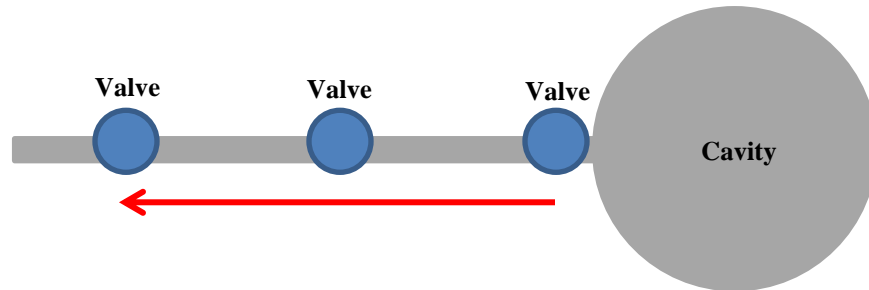


Figure 6-3 Valve position guideline for a new simulation

From a design aspect, the current Melt modulation system is working with DME mold presented in Chapter 4. To conduct an experiment, the whole mold with the compact system inside needs to be assembled into the Nissei machine. It takes a long setup time if there is another mold already on the machine. The new Melt modulation system which is compatible with DME's MUD type helps reduce setup time because only the mold insert needs to be changed. Another concept to improve Melt modulation system design is to make the system easier to attach or detach to the mold. Since the current compact system is embedded to the deepest part of the mold, a user needs to disassemble all mold parts in order to change any configuration of the control valve system. The easy-attach concept provides more choice to manufacturer with a decision to use Melt modulation system or not with the same cold runner system.

The application used to control Melt modulation system was created by Delphi 7 for many years. The application can run only on Windows XP which starts to be out of date. The

new application should be written so that the actuator can be controlled by any computer in the campus. If the new experiment only focuses on on-off positions, the new Melt modulation system can be driven using a simpler actuator such as a pneumatic rotary actuator.

Another aspect that can be developed is force analysis. Since the invention of Melt modulation technology, the torque needed to rotate the control valve has never been calculated. Because the valve has to rotate when the runner is filled to control packing pressure, it is necessary to know the torque that can overcome the pressure applied from a machine and high viscosity melt flow when it starts to solidify. Fortunately, the actuator presented in Chapter 4 is strong enough to hold the valve position for a common process run by the Nissei machine, but it might not work with a bigger machine which can produce higher packing pressure. Thrust load on the valve port has to be determined too. High thrust load can cause damage to an actuator directly connected to the valve stem or a case which is attached to the mold.

6.3 Conclusion Remarks

The expansion of the capability of the Melt modulation technique to the packing stage has been started in this research and produced a convincing result. All three objectives which were proposed have been accomplished. Controlling packing parameters will definitely change the optical quality of polymeric products. The new cold runner system and new Melt modulation configuration were fabricated in order to test with packing stage control applications. At last the initial investigation of the valve capability has been done.

With a development of Melt modulation hardware and an extended capability, the Melt modulation technique is now more functional and able to apply to a wider area of the

injection molding industry. These reasons make Melt modulation technology more attractive for an investment. The proposed future work will continuously provide a solid knowledge which helps an engineer understand Melt modulation techniques better. Adding with the new design and process development in the future, Melt modulation technique will enhance the injection molding process to the next level and be another solution for the industry.

REFERENCES

1. Beaumont, J. P., 2004, *Runner and Gating Design Handbook*, Carl Hanser Verlag, Munich.
2. Tantrapiwat, A., 2009, "Melt Modulation Systems for Enhanced Polymer Processing," Ph.D. dissertation, Lehigh University, Bethlehem, PA.
3. Layser, G. S., 2007, "An Investigation of Controlled Melt-Manipulation Based Dynamic Injection-Molding Processes," Ph.D. dissertation, Lehigh University, Bethlehem, PA.
4. Beaumont, J. P., Nagel, R., and Sherman, R., 2002, *Successful Injection Molding*, Carl Hanser Verlag, Munich.
5. Rosato, D. V., Rosato, D.V., and Rosato, M. G., *Injection Molding Handbook*, 3rd edition, Kluwer Academic Publishers.
6. Kazmer, D., and Barkan, P., 1997, "Multi-Cavity Pressure Control in the Filling and Packing Stages of the Injection Molding Process," *Polymer Engineering and Science*, **37**(11), pp. 1865-1879.
7. Kazmer, D., and Barkan, P., 1997, "The Process Capability of Multi-Cavity Pressure Control for the Injection Molding Process," *Polymer Engineering and Science*, **37**(11), pp. 1880-1895.
8. Harry, D. H., 1974, "Direct Cavity Pressure Control of Injection Molding," **20**, pp. 53-55.
9. Park, H. P., Rhee, B. O., and Cha, B. S., 2006, "Varial-Runner System for Family Mold Filling Balance," *Solid State Phenomena*, **116-117**, pp. 96-101.
10. Hitec RCD USA, Inc., "HSR-5990TG HMI Ultra Premium Robot Servo," from <http://www.hitecrcd.com/products/digital/robotics/hsr-5990tg.html>
11. DME Company LLC, "9-7/8 × 8" A-Series Mold Bases," pp. 54-55.
12. Vishay Measurement Group, from <http://www.vishay.com>
13. Baumer, S., 2005, *Handbook of Plastic Optics*, Wiley-VCH, Weinhiem.
14. Plastic Optics, "Optical Reference Guide," from <http://www.plasticoptics.com/referenceguide.html>

15. Wang, P. J., and Lai, H. E., 2007, "Study of Residual Birefringence in Injection Molded Lenses," ANTEC, pp. 2494-2498.
16. Li, H., and Peng, Y., Turng, L. S., and Wang, X., 2009, "Research on Residual Stresses of Injection Molded PC Parts," ANTEC, pp. 1689-1693.
17. Pantani, R., Coccorullo, I., Speranza, V., and Titomanlio, G., 2007, "Morphology Evolution during Injection Molding: Effect of Packing Pressure," Polymer, **48**(9), pp. 2778-2790.
18. Li, H., Jiang, K., Xu, W., and Shen, Ch., 2007, "Effect of Processing Parameters on Optical Properties of Injection Molded Polystyrene Parts," ANTEC, pp. 590-594.
19. Hu, G. H., and Cui, Z. S., 2010, "Effect of Packing Parameters and Gate Size on Shrinkage of Aspheric Lens Parts," J. Shanghai Jiaotong University, Shanghai, **15**(1), pp. 84-87.
20. Wang, T. J., and Yoon, C. K., "Effects of Process Conditions on Shrinkage and Warpage in the Injection Molding Process," ANTEC, pp. 584-593.
21. Tsai, K. M., Hsieh, C. Y., and Lo, W. Ch., 2009, "A Study of the Effects of Process Parameters for Injection Molding on Surface Quality of Optical Lenses," Material Processing Technology, pp. 3469-3477.
22. ODN, "ASTM D638," from <http://www1.odn.ne.jp>
23. Nissei Coporation, "PS40E5ASE Inj. Molding Machine Specifications,"
24. Moldflow technical information document
25. Change, C. W., Hsu, C. H., and Chen, C. H., 2008, "The Effects of Different Process Conditions on the Quality of Injection-Molded Parts," ANTEC, pp.2401-2404.
26. INEOS NOVA LLC, "Polystyrene Technical Bulletin," from <http://www.ineosstyrenics.net/media/pdf/tech-docs/ps101-1008polystyreneinjectionmolding.pdf>
27. Kistler Instrumente AG, 2007, "Mold Cavity Pressure Sensor Type 6159A"
28. Robotzone, LLC., "Servo to Shaft Couplers," from http://www.servocity.com/html/servo_to_shaft_couplers.html

29. DME Company LLC, “INCH High-Hardness Ejector Pins – H13 Nitrided - Straight,” pp. 246.
30. Altuglas Internation, Arkema Group, “Plexiglas® Acrylic Molding Resin,” from <http://www.plexiglas.com/acrylicresin/technicaldata/injectionmolding>
31. IDES The Plastic Web®, “Polycarbonate (PC) Processing Information,” from http://www.ides.com/generics/PC/PC_processing_information.htm
32. AmericasStyrenics, LLC., 2011, “Styron® 685D,” from <http://www.amstyrenics.com>

VITA

Punlop Teeraparpwong was born on January 11th, 1987 to Phayoung and Roongthip Dhirapharbwongse. He grew up in Bangkok, Thailand and studied at Bangkok Christian College until he got high school diploma. Then he attended Chulalongkorn University and graduated with B.E. in Mechanical Engineering in May 2009. After receiving Bachelor degree, Punlop continued to pursue Masters degree in Mechanical Engineering, Lehigh University.